

Development of a mathematical model for the
occupancy of mRNA with ribosomes in
Saccharomyces cerevisiae

Jannis Uhlendorf

Bachelor Thesis



Freie Universität Berlin
Department of Mathematics and Computer Science
Bioinformatics Program

Advisors:
Professor Dr. Edda Klipp
Professor Dr. Per Sunnerhagen

Max Planck Institute for Molecular Genetics
Innstraße 63-73
14195 Berlin
Germany

Email: uhlendorf@molgen.mpg.de

June 6th - August 1st 2006

Abstract

This thesis describes the development of a mathematical model for the occupancy of mRNA with ribosomes in the yeast *Saccharomyces cerevisiae*. The model is supposed to describe the change in polysomal association of mRNA, that is found when yeast cells are subjected to a hyperosmotic shock. A hyperosmotic shock is a rapid increase of the osmolarity of the surrounding media of a cell. Yeast cells respond with a variety of changes to hyperosmotic shock, including a down regulation of the translational apparatus. This means that the number of ribosomes an average mRNA has bound decreases. In this thesis different models to simulate this behavior are developed, and tested for their properties and their ability to describe the translational downregulation after osmotic shock.

Inhalt

Diese Arbeit beschreibt die Entwicklung eines mathematischen Modells für die Beladung von mRNA mit Ribosomen in der Hefe *Saccharomyces cerevisiae*. Das Modell soll die Änderung der polysomalen Assoziierung von mRNA beschreiben, wenn Hefezellen einen hyperosmotischen Schock erfahren. Ein hyperosmotischer Schock ist eine schnelle Zunahme der Osmolarität des umgebenden Mediums einer Zelle. Hefezellen reagieren mit einer Vielzahl von Änderungen auf einen hyperosmotischen Schock, unter Anderem mit einer Herabregelung der Translation. Dies bedeutet, daß die Zahl der Ribosomen, die eine durchschnittliche mRNA gebunden hat abnimmt. In dieser Arbeit werden verschiedene Modelle entwickelt um dieses Verhalten zu beschreiben und auf ihre Fähigkeit hin getestet, die osmotische Stressantwort von Hefezellen zu beschreiben.

Acknowledgements

First of all I would like to thank my supervisors Edda Klipp and Per Sunnerhagen for not only making this work possible, but also for their great support and the many vital comments on my work. In addition I would like to thank Malin Hult for her brilliant explanations that were essential for this work. Thank you, Malin and Per for providing me with the data this work is based on. Also, I would like to thank Axel Kowald, Jörg Schaber and Wolf Liebermeister for a lot of ideas and comments on my work, and Katharina Albers, Matteo Barberis, and Marvin Schulz for carefully proof reading the manuscript.

Contents

Summary	2
Preface	3
1 Introduction	1
1.1 Objective	1
1.2 Modeling biological processes	1
1.2.1 Mathematical description	2
1.3 Biological basis	3
1.3.1 Gene expression in eukaryotes	3
1.3.2 Osmoadaption in yeast	8
1.3.3 Sensing and signaling osmotic changes	8
1.4 Methods	10
1.4.1 DNA Microarrays	10
1.4.2 Analysis of polysomes	11
1.4.3 Gillespie algorithm for stochastic simulation	13
1.4.4 Differential Evolution algorithm for optimization	15
2 Model construction	17
2.1 Models	17
2.1.1 Single rate model	17
2.1.2 Multiple rate model	17
2.1.3 Bitstring model	18
2.1.4 mRNA degradation and production	18
2.1.5 Degradation and production of ribosomes	19
3 Model analysis	20
3.1 Mathematical analysis	20
3.1.1 Single rate model	20
3.1.2 Multiple rate model	22
3.1.3 Bitstring model	23
3.2 Simulation analysis	24
3.2.1 Single rate model	25
3.2.2 Multiple rate model	26
3.2.3 Bitstring model	28

4	Data fit	31
4.1	Data	31
4.2	Used tools	31
4.2.1	SBMLpet	32
4.2.2	Berkeley Madonna	32
4.2.3	Matlab	33
4.3	Steady state fit	34
4.3.1	Single rate model	34
4.3.2	Multiple rate model	35
4.3.3	Bitstring model	37
4.4	Time course fit	40
4.4.1	Multiple rate model	40
4.4.2	Model with 3 initiation rates	42
5	Results	47
5.1	Comparison	47
5.1.1	Models	47
5.1.2	Processes	48
5.2	Validation	49
5.3	Conclusions	54
A	Proofs	55
A.1	Derivation of fomulae (3.5) and (3.6)	55
A.2	Derivation of formula (3.7)	56
B	Deterministic simulation in MATLAB	58
	Bibliography	61

Abbreviations

Abbreviation	Meaning or Context
BM	Berkeley Madonna
Cdc24	HOG Pathway
Cdc42	HOG Pathway
CPSF	Cleavage and Polyadenylation Factor (Transcription Termination Factor)
CstF	Cleavage Stimulation Factor F (Transcription Termination Factor)
eEF-1A	Translation Elongation Factor
eEF-2	Translation Elongation Factor
eIF-2	Translation Initiation Factor
eIF-2B	Translation Initiation Factor
eIF-4A	Translation Initiation Factor
eIF-4E	Translation Initiation Factor
eIF-4G	Translation Initiation Factor
ER	Endoplasmatic Reticulum
eRF-1	Translation Release Factor
eRF-3	Translation Release Factor
Fps1p	Glycerol Channel
DE	Differential Evolution
HOG	High Osmolarity Glycerol
Hog1	HOG Pathway
MAP	Mitogen Activated Protein
MAP-KK	MAP Kinase Kinase
MAP-KKK	MAP Kinase Kinase Kinase
MCA	Metabolic Control Analysis
miRNA	Micro RNA
mRNA	Messenger RNA
ODE	Ordinary Differential Equation
PAF	Polysomal Association Factor
Pbs2	HOG Pathway
pre-mRNA	Premature Messenger RNA
rRNA	Ribosomal RNA
RSSQ	Residual Sum Of Squares
SBML	Systems Biology Markup Language
Sho1	HOG Pathway
Sln1	HOG Pathway
snoRNA	Small Nucleolar RNA
snRNA	Small Nuclear RNA
Ssk1	HOG Pathway
Ssk2	HOG Pathway
Ssk22	HOG Pathway
Ste11	HOG Pathway
Ste20	HOG Pathway
Ste50	HOG Pathway
TFIIA	Transcription Initiation Factor
TFIIB	Transcription Initiation Factor
TFIID	Transcription Initiation Factor
TFIIE	Transcription Initiation Factor
TFIIF	Transcription Initiation Factor
TFIIH	Transcription Initiation Factor
tRNA	Transfer RNA
UTR	Untranslated Region
UV	Ultraviolet
Ypd1	HOG Pathway

List of Tables

3.1	Parameters for simulation 3.5	28
4.1	Parameters for steady state fit - single rate model	35
4.2	Parameters for steady state fit - multiple rate model	38
4.3	Parameters for steady state fit - bitstring model	39
4.4	Parameter $k_{transcr}$ for time course fit - multiple rate mRNA production A . .	41
4.5	Parameters for time course fit - multiple rate ribosome degradation A	42
4.6	Parameters for time course fit - multiple rate model initiation rate change	44
4.7	Parameters for time course fit - multiple rate model mRNA production B	45
4.8	Parameters for time course fit - multiple rate model ribosome degradation B . .	46

List of Figures

1.1	Gene expression in eukaryotes	4
1.2	Map of the HOG pathway	9
1.3	Example of polysomal profile	12
1.4	Different methods for polysomal profiling	13
3.1	Single rate model: Plot of X against mRNA concentrations	21
3.2	Single rate model: Simulation of ribosome degradation	22
3.3	Simulation of single rate model	25
3.4	Multiple rate model Simulation A	26
3.5	Multiple rate model Simulation B	27
3.6	Multiple rate model polysome distribution	28
3.7	Bitstring model simulation A	29
3.8	Bitstring model simulation B	30
4.1	Example of polysomal profile	32
4.2	Goodness of fit Berkeley Madonna	33
4.3	Goodness of fit - single rate model time point 0	36
4.4	Goodness of fit - single rate model time point 10	37
4.5	Goodness of fit - bitstring model time point 0	39
4.6	Goodness of time course fit - multiple rate model mRNA production A	41
4.7	Goodness of time course fit - multiple rate model ribosome degradation A	43
4.8	Goodness of time course fit - multiple rate model initiation rate change	44
4.9	Goodness of time course fit - multiple rate model mRNA production B	45
4.10	Goodness of time course fit - multiple rate model ribosome degradation B	46
5.1	Change in the polysomal association factor after osmotic shock for different types of genes	50
5.2	PAF simulation for bistring model	51
5.3	Simulation bitstring model upregulated mRNA	52
5.4	Simulation bitstring model downregulated mRNA	53
5.5	Simulation bitstring model not regulated mRNA	53
B.1	MATLAB code for gradient function	59
B.2	MATLAB code for simulation	60

Chapter 1

Introduction

1.1 Objective

The aim of this work has been to develop a mathematical model, that explains the change in the polysomal association of mRNAs in *Saccharomyces cerevisiae* when subjected to osmotic stress. Yeast cells that are transferred to a medium of high osmolarity show a specific response (Hohmann, 2002), which includes the global downregulation of the translational apparatus. This means that the polysomal profile of the cells, is shifted from a distribution consisting of highly translated mRNAs (polysomes) to a distribution formed by lower translated mRNAs.

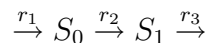
In this work different models for the occupancy of mRNA with ribosomes have been developed and tested for their ability to describe both, the distribution of polysomes in unstressed cells, and the temporal change in the polysomal pattern after osmotic shock. For this purpose different processes that may cause the change in the translation state in response to osmotic shock have been incorporated in the different model, and examined for their influence on these models.

1.2 Modeling biological processes

Systems Biology attempts to understand the biology at system level (Kitano, 2002). This means understanding the system in general, rather than focusing on isolated subsystems. Because of the complexity of living organisms, which dooms unstructured attempts to globally understand them to fail, this approach can only be successful by making use of a general mathematical description of the underlying processes. Methods for the global mathematical analysis of reaction systems have been developed, for instance the metabolic control analysis (MCA) allows to determine the influence of single reactions or metabolites on the whole reaction system (Kacser and Burns, 1973; Heinrich and Rapoport, 1974). For the mathematical description of reaction systems a general approach exists, which shall be described in the following section.

1.2.1 Mathematical description

The mathematical description of a reaction system can be formulated in a general way (Klipp et al., 2005a). First of all, the topology of the network can be described by the *stoichiometric matrix*. The stoichiometric matrix N consists of a column for each reaction and a row for each substrate. The element n_{ij} is the stoichiometry at which the i th substrate participates in the j th reaction, or 0 if the substrate does not take part in this reaction. The simple reaction system



leads to the stoichiometric matrix

$$N = \begin{pmatrix} 1 & -1 & 0 \\ 0 & 1 & -1 \end{pmatrix}$$

The concentration change of a metabolite in time is the sum of the concentration changes that are caused by the particular reactions, in which the metabolite participates. Therefore, the concentration change of a metabolite is given by its row in the stoichiometric matrix multiplied with the vector of reaction velocities v . This can be written in as:

$$\frac{dS_i}{dt} = \sum_{j=1}^r n_{ij} \cdot v_j \quad (1.1)$$

where v_j denotes the reaction velocity of the j th reaction.

The substrate concentrations also can be collected in a vector S , where s_i denotes the concentration of substrate i . The reaction velocity vector v generally depends on the concentration of all metabolites S and the parameters p , which can be written as $v = v(S, p)$.

Equation (1.1) can be written in matrix notation as:

$$\frac{dS}{dt} = Nv = Nv(S, p) \quad (1.2)$$

To investigate the properties of such a model, it is generally considered to be in steady state, which means that none of the substrate concentrations changes over time. A concentration change for one of the metabolites would mean that this substrate is either removed from the system, or accumulated. This cannot be if the system is balanced. The steady state assumption can be written in mathematical terms as:

$$\frac{dS}{dt} = Nv = 0 \quad (1.3)$$

Solving this equation for the reaction velocities v gives the fluxes J that can be reached in steady state. The fluxes J differ from the reaction velocities, in the point that they only depend on the parameters p , not on the concentrations S .

$$J(p) = v(S, p) \quad (1.4)$$

Solving Equation (1.3) for the metabolite concentrations gives the metabolite concentrations $S(p)$ that can be reached in a steady state, in dependence of the parameters p . Unfortunately, in most of the cases it is not possible to solve Equation (1.3) analytically.

Equation (1.2) gives a deterministic description of the reaction system, which means that for known initial concentrations S and parameters p , the concentrations can be determined for every proximate time point by integrating this equation over the time. This can be done analytically to get a general mathematical description, if the system is not too complicated, or numerically to simulate the system.

The deterministic approach requires that (i) the system is well mixed, and (ii) the molecule numbers are high. For small molecule numbers also stochastic processes play a role, since molecule numbers can only adopt discrete values. A stochastic description of a reaction system gives the probability for each possible way in which the system can evolve. A way in this context is made up by the concentrations of all metabolites at all time points. A stochastic simulation chooses one possible way in which the system could evolve, but does this according to the probability that the system will evolve in this direction.

1.3 Biological basis

1.3.1 Gene expression in eukaryotes

Gene expression denotes the process of converting information, that is contained in the DNA sequence of a gene, into structural or signaling elements of the cell. These elements are proteins in most cases, but can also be RNAs. In *Saccharomyces cerevisiae*, for example, more than 700 of its roughly 6000 genes produce RNA as their final product (Eddy, 1999; Goffeau et al., 1996). When we speak of RNA, we usually mean the messenger RNA (mRNA) that serves as a template for protein synthesis. But there exist also a variety of other RNA types in the cell, which are termed after their function. The most important noncoding RNAs are ribosomal RNAs (rRNA), which are an essential part of the ribosome, transfer RNAs (tRNA), which serve as adaptors between the mRNA and amino acids during translation, microRNAs (miRNA) which are thought to regulate the expression of other genes, small nuclear RNAs (snRNA), which among other things play an important role during splicing, and small nucleolar RNAs (snoRNA), which process rRNAs. In eukaryotes, the different types of mRNA are produced by three different RNA-polymerases.

The process of gene expression for protein coding RNAs is displayed in Figure 1.1. In the first step, a region on the DNA called transcription unit is transcribed to a complementary RNA. The catalyzing enzyme is the RNA-polymerase II, and the RNA product is called premature messenger RNA (pre-mRNA). This pre-mRNA undergoes several modifications, before it is engaged in protein synthesis (Lewis and Tollervey, 2000). The first modification is the addition of a modified guanine nucleotide at the 5' end, which already takes place during transcription. This cap is important for the binding of ribosomes to the designated mRNA. On the other end of the pre-mRNA a set of adenosine residues is added, forming a so called polyA tail, which

determines the stability of the mRNA and serves as an export signal from the nucleus (Huang and Carmichael, 1996; Drummond et al., 1985). The third modification is called splicing and denotes a process in which noncoding regions of the mRNA are excised. This process is catalyzed by a RNA-protein complex called spliceosome, which cuts out the noncoding regions (introns) in a two step process. By varying the number and positions of splice events, a process called alternative splicing, it is possible also for a eucaryotic cell to encode different proteins on a single gene (Black, 2000). Another optional modification is the change of the nucleotide composition of the mRNA, called RNA editing.

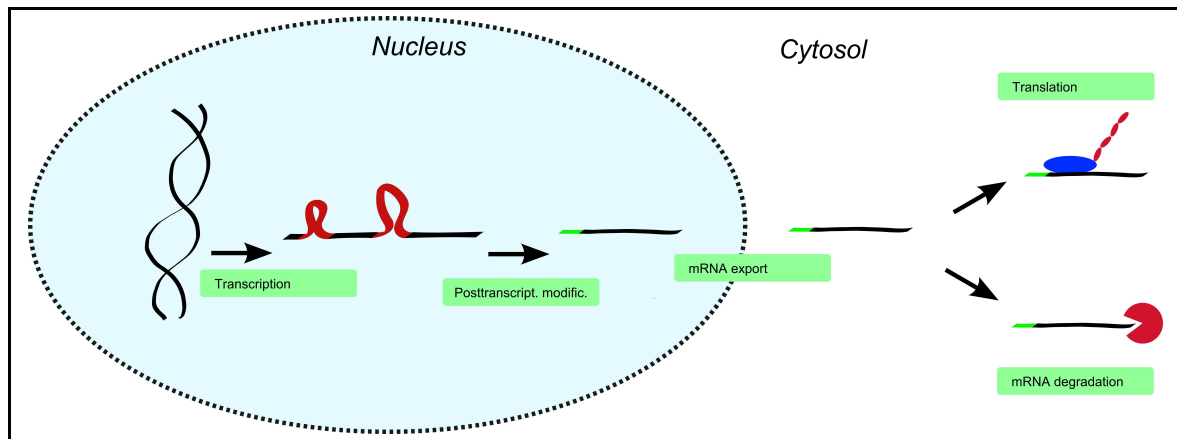


Figure 1.1: Gene expression in eukaryotes

After the pre-mRNA has undergone the above described post transcriptional modifications, it is a mature mRNA and ready to be exported to the cytosol. This export is highly selective to ensure that only correct processed mRNAs are translated. The nuclear pore complex recognizes several indications for the processing state of an mRNA, and exports only mature mRNAs (Daneholt, 1997). In the cytosol ribosomes bind to the 5' cap of the mRNA and translate its base sequence into the amino acid sequence of a protein. The synthesis of all proteins takes place in the cytosol. Proteins that contain a special signal sequence are recruited to the endoplasmic reticulum (ER) during translation, where the ribosome synthesizes the protein directly into the ER lumen. In the ER proteins are further processed by the addition and trimming of oligosaccharides before they are passed on to the golgi apparatus, which is also involved in the oligosaccharide processing, and finally sorts and packages the proteins for further transport.

It is important to mention that the above described processes correspond to eukaryotic cells. In bacteria the processes are somewhat easier, although they are similar. Fundamental differences are the absence of post transcriptional modifications, the use of just one RNA polymerase, and the potential to encode more than one protein on one mRNA in prokaryotes. For further details on the described biological processes see (Alberts et al., 2002).

Since the cell has to be able to control its protein synthesis, another fate of the cytoplasmic mRNAs is the degradation by ribonucleases. The degradation rate of different mRNAs depends

on the type of the mRNA (Lowell et al., 1992) as well as on the environmental and intrinsic conditions of the cell (Bernstein and Ross, 1989; Zingg et al., 1988).

Cells have to be able to alter their gene expression because of specialization in a multicellular organism, and in response to environmental changes. These differences in mRNA and protein levels occur not due to changes in the DNA sequence, but are controlled by a variety of mechanisms that intervene in processes during or downstream to transcription (Gurdon, 1968). The regulation of gene expression can be roughly divided into transcriptional and post transcriptional control mechanisms.

Transcriptional control mechanisms

The transcription is classified into the three steps: initiation, elongation, and termination. Each of these steps requires not only the RNA polymerase, but a large number of helping proteins named transcription factors.

Initiation starts with the binding of the general transcription factor TFIID to a region, typically located 25 nucleotides upstream from the transcription start, called TATA box. The binding of TFIID causes the binding of several other transcription factors (TFIIA, TFIIB, TFIIIE, TFIIIF, and TFIIH) as well as the RNA polymerase II (Conaway and Conaway, 1993). TFIIH plays an important role in unwinding the RNA and in the activation the polymerase by phosphorylation. Altogether, well over 100 subunits are involved in transcription initiation. To assemble this huge machinery a mediator protein complex is required. This mediator binds to a specific DNA sequence, thereby activating the transcription for a specific gene.

After the initiation most of the initiation factors dissociate, and elongation factors bind to the polymerase. These elongation factors reduce the probability of dissociation of the polymerase from the RNA. Likewise are termination factors required, that recognize the polyadenylation site in the growing RNA, thereby terminating the elongation process. The termination factors cleavage stimulation factor F (CstF) and cleavage and polyadenylation factor (CPSF) recognize the termination signal in the growing RNA sequence, and as their name indicates trigger the cleavage of the mRNA chain and the addition of a poly-A tail, which is catalyzed by the poly-A polymerase. The poly-A tail is bound by poly-A binding proteins.

Regulation of transcription is possible at various of the described steps. First of all, the initiation of transcription often requires the remodeling of the chromatin structure of the DNA to facilitate binding of the polymerase to the DNA. This task is fulfilled by chromatin remodeling complexes, which can be selectively brought to specific regions of the DNA, thereby activating specific genes (Kingston, 1999). Other gene regulatory proteins bind to specific DNA sites, thereby either activating genes by attracting general transcription factors or the polymerase to the DNA region (enhancers), or inhibiting the formation of the initiation complex (repressors) (Kornberg, 1999). Besides the regulation of initiation, there exist also proteins that regulate the rate of elongation (Bentley, 1995). A mechanism that is only present in vertebrates is the methylation of DNA regions, which leads to the binding of proteins, which remodel the chromatin structure, making the DNA transcriptionally inactive.

Of course most gene regulatory proteins do not act on their own, but are then again regulated upstream signaling pathways.

Post transcriptional control mechanisms

Post transcriptional control includes all the gene regulatory processes that occur after transcription. One way of post transcriptional control is the above mentioned alternative splicing process, where certain splice sites are left out, or cryptic splice sites are activated. This alternative splicing does not exclusively occur by chance, but is also regulated by other molecules in both positive and negative way.

As also noted above, the coding sequence of mRNA can be changed by enzymes after transcription in a process called RNA editing.

Another way to regulate the translation rate of mRNAs is the control of export from the nucleus, since protein synthesis only takes place in the cytosol. To be exported, an mRNA needs to be correctly capped, polyadenylated, and spliced. This mechanism is known to play a role in stress induced differential gene expression (Saavedra et al., 1996).

Furthermore, the distribution of mRNAs over the cytoplasm is not random, but a regulated process (Ding and Lipshitz, 1993; Singer, 1992; Wilhelm and Vale, 1993). This is an economic way of the cell to direct proteins to their destination, as it only requires the transport of the mRNA instead the produced proteins. The signals directing the mRNA localization are usually found in the 3'-UTR of the mRNA.

The translation of mRNAs is also controlled by the cell. Several proteins for example bind to the 5' end of the mRNA, thereby inhibiting the translation initiation. Other proteins bind to the 3' poly-A tail and disturb the communication between the 5' cap and the 3' poly-A tail, which is required for efficient translation. Global regulation of the protein synthesis rate can be achieved by the phosphorylation of the initiation factor eIF-2 (Wek, 1994), which normally mediates the binding of the methionyl-tRNA to the 40S ribosomal subunit. Phosphorylation of eIF-2 enhances its affinity to eIF-2B, which is required for eIF-2 to release its bound GDP after the initiation process. This leads to the consumption of eIF-2B, thereby arresting the reactivation of eIF-2 which again induces a lower initiation rate.

A very important way for the cell to regulate the expression of certain genes is the degradation rate of the corresponding mRNAs. It has been shown that the half-lives of mRNAs vary from less than one minute to more than one hour (Herrick et al., 1990; Jacobson et al., 1990), what indicates a contribution of this mechanism to differential gene expression. The polyA tail plays an important role in this pathway (Wilson et al., 1978). In the cytosol the polyA tail is shortened continuously by exonucleases, and once the length of the polyA tail falls below a threshold a degradation pathway is triggered. This degradation pathway involves the removal of the 5' cap in a process called decapping and the subsequent degradation of the mRNA. The proteins that shorten the polyA tail compete in general with the translational apparatus, wherefore a well translated mRNA is subjected to a lower degradation than a less translated one (Prieto et al., 2000). The degradation of the polyA tail is also thought to be influenced

by proteins, that bind to specific sequences in the 5' UTR. There exist a second pathway for mRNA degradation in which an exonuclease cleaves away the polyA tail, which lead again to degradation of the mRNA. mRNAs which are degraded in this way carry a special signal in their 5' UTR. For a comprehensive review on post transcriptional control see (McCarthy, 1998).

Translation

The translation is the process of decoding the nucleotide sequence of an mRNA into a protein's primary structure. The location of translation is the cytoplasm, so the mRNA has to be exported from the nucleus in advance. The initiation of translation begins with the binding of the initiator tRNA, which carries methionine, to the small ribosomal subunit. This requires also the binding of the eucaryotic initiation factor eIF-2. After that the small ribosomal subunit binds to the 5' cap of the mRNA, whereby the selective binding of the cap is achieved by the initiation factor eIF-4E. For the binding of the 40S ribosomal subunit and eIF-4E also eIF-G is required, which is supposed to mediate the binding of the ribosomal subunit and to enhance the cap binding of eIF-4E (Ptushkina et al., 1998). After the binding to the cap, the complex, consisting of the 40S subunit and the initiation factors, moves along the 5' untranslated region (5' UTR) until it encounters an AUG start codon. This searching may be driven by the initiation factor eIF-4A (Sonenberg, 1996). Once the complex has found an AUG codon, the initiation factors dissociate and the big 60S ribosomal subunits binds to form the complete 80S ribosome. The nucleotides surrounding the AUG codon influence the efficiency of the AUG recognition, thereby providing a mechanism to code more than one protein even on a eukaryotic mRNA.

The ribosome has three binding sites for tRNAs, the aminacyl-tRNA-site (A), the peptidyl-tRNA-site (P), and the exit-site (E). After the formation of the ribosome, the methionine-tRNA is bound to the P-site. During elongation the tRNA that matches the next codon binds to the A-site, allowing the ribosome to catalyze a peptide bond between its bound amino acid and the growing peptide chain. During this reaction the new tRNA moves from the A-site to the P-site, while the preceding tRNA moves to the E-site, where it is released. At this time the tRNA is located in the P-site, and holds the growing peptide chain covalently linked, while the A-site is vacant and can be accessed by the next tRNA. As for the initiation various elongation factors are required for the elongation process. eEF-1A forms a complex with GTP and aminoacyl-tRNA, facilitating the binding to the ribosome. eEF-2 helps in translocating the peptidyl-tRNA to the P site, and is likely to be regulated in higher cells (Pain, 1996; Nairn and Palfrey, 1996)

Termination of the translation process is induced by the occurrence of one of the stop codons (UAA, UAG, or UGA), which have no matching tRNAs, but instead trigger the binding of the release factors eRF-1 and eRF-3 to the A-site. The release factors initiate the release of the peptide chain by the addition of water, and the disaggregation of the ribosome.

Because the translation of an average mRNA takes longer than it takes for the next initiation process to take place, mRNAs are not only transcribed by a single ribosome, but instead form a complex with several ribosomes called polyribosomes (or polysomes).

1.3.2 Osmoadaptation in yeast

The osmolarity of the surrounding media is very important for a cell, since it determines its turgor pressure. Osmolarity is a measurement for the amount of solutes per litre of solution. Because the interior of a cell has generally a higher osmolarity than the surrounding medium, there is a constant force driving water into the cell to offset this imbalance. This force leads to an antagonizing force arising from the limited expansion ability of the plasma membrane and the cell wall, which is called turgor pressure (Blomberg and Adler, 1992; Wood, 1999).

Since the osmolarity of the medium surrounding the cell can change, a cell has to be able to respond to those changes in order not to shrink or to burst. When cells are subjected to a so called hyperosmotic shock, which is a rapid upshift of the extracellular osmolarity, they have to deal with water outflow and consequent cell shrinkage. On the other hand, a hypoosmotic shock (osmotic downshift) leads to water influx and thereby to increased turgor pressure. The cell senses osmotic changes by certain receptors, and relays them through different signaling pathways to alter gene expression and the production and transport of certain metabolites. A mathematical model for the osmotic stress response of yeast is available (Klipp et al., 2005b), but this model does not include the occupancy of mRNA with ribosomes. A very comprehensive review about the signaling and response of yeasts to osmotic stress has been written by Stefan Hohmann (Hohmann, 2002).

1.3.3 Sensing and signaling osmotic changes

There exist several proteins sensing osmotic changes. They either act similar to chemosensors, with the difference that they are not restricted to a certain compound, or sense mechanical changes that result from the osmotic shift. In *Saccharomyces cerevisiae* the Sln1 and Sho1 proteins are the most prominent osmotic sensors, both controlling the high osmolarity glycerol (HOG) pathway (see Figure 1.2).

The Sln1 pathway is active under low osmolarity conditions, where it acts by inhibiting the HOG pathway. The signal transduction from Sln1 to HOG1 can be divided in two modules, a two component phosphorelay module, and a mitogen activated protein (MAP) kinase module. The two component module is actually a three component system comprising the proteins Sln1, Ypd1 and Ssk1. The two component in the name indicates the similarity of the module to classical procaryotic two-component transduction systems (Widmann et al., 1999). Sln1 has an autophosphorylating activity, which is active under normal osmotic conditions, and is inhibited by high osmolarity. The autophosphorylation of Sln1 implicates the phosphorylation of Ypd1, which again transfers the phosphate group to Ssk1. Ssk1 stimulates the downstream MAP kinase module by the phosphorylation of Ssk2 and Ssk22, but is inactivated by phosphorylation. Thereby, high osmolarity activates the pathway by dephosphorylation of Ssk1.

The following MAP kinase module consists of the four components: Ssk2, Ssk22 (both MAP kinase kinase kinase (MAP-KKK)), Pbs2 (MAP kinase kinase (MAP-KK)), and Hog1 (MAP kinase). Hog1 then again activates several factors that are important for the stress response. MAP kinase signaling cascades generally consist of three proteins, that amplify an incoming

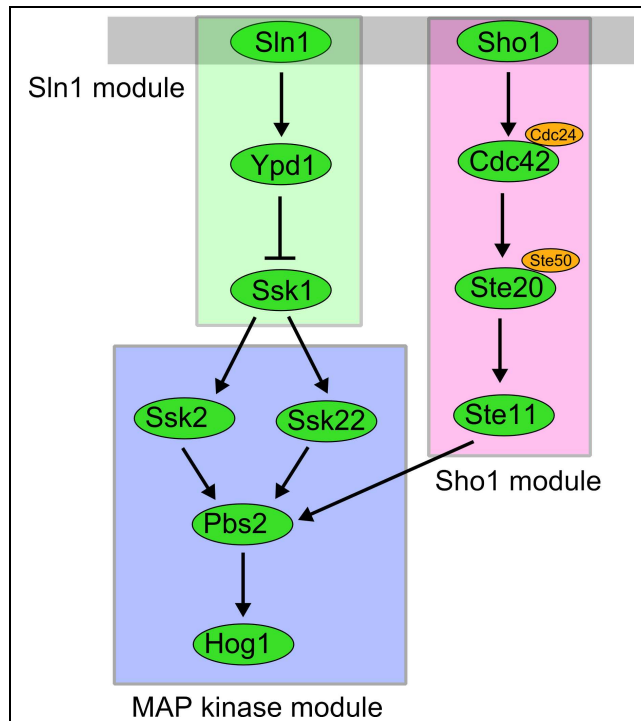


Figure 1.2: Map of the HOG pathway

signal by passing on phosphorylation signals. A simple three component MAP kinase cascade would consist of an MAP-KKK element, which is activated by an activator (e.g a receptor) and thereupon phosphorylates the MAP-KK. In the phosphorylated state MAP-KK activates the protein MAP-kinase (by phosphorylation), which activates certain effector proteins affecting their activity.

In addition to the Sln1 pathway, yeast cells activate the MAP kinase module by another osmotic sensor, the Sho1 pathway (Helliwell et al., 1994). Sho1 is active under high osmolarity conditions and activates the G-Protein Cdc42, which relays the signal to kinase Ste20, that again activates the MAP-KKK Ste11. This reaction sequence also requires Cdc24, the exchange factor for Cdc42, and Ste50 (Raitt et al., 2000). Ste20 is a MAP-KKK and activates the MAP-KK Pbs2 in the MAP kinase module, thereby converging the two pathways.

Response to osmotic changes

When the cell is subjected to a rapid osmotic upshift, it shrinks within seconds to a fraction of its initial volume (Albertyn et al., 1994).

Consequences of osmotic upshift include an enhanced production of glycerol and trehalose, and the reduction of glycerol export. Glycerol is a very important osmoactive substance in the cell, and increased cellular concentration of glycerol can countervail the increased external osmolarity. The glycerol metabolism is effected quite dramatically by hyperosmotic shock, as the genes for glycerol synthesis (GPD1 and GPP2) transiently increase up to about 50-fold

(Albertyn et al., 1994; Hirayarna et al., 1995; Norbeck et al., 1996). In addition, Fps1p, a cell wall channel for glycerol, is regulated negatively in response to hyperosmotic shock (Tamas et al., 1999; Luyten et al., 1995).

General pathways of the cell such as amino acid metabolism, cell wall maintenance, nucleosome structuring, DNA synthesis, and nucleotide metabolism are downregulated under osmotic stress (Hohmann, 2002). In addition, the elongation step of protein synthesis is also believed to be downregulated by osmotic stress (Teige et al., 2001).

Also the production of trehalose and glycogen is found to increase in response to (not exclusively) osmotic stress (Causton et al., 2001; Gasch et al., 2000). Trehalose is a disaccharide which is important for cells to survive under stress (Deschenes et al., 1999; Estruch, 2000; Francois and Parrou, 2001; Nwaka et al., 1995; Singer and Lindquist, 1998), and glycogen is a polysaccharide which serves as a energy storage in the cell. However, the increased production of trehalose does not accumulate it in the cell (Hounsa et al., 1998), which is due to likewise increased degradation.

1.4 Methods

1.4.1 DNA Microarrays

DNA microarrays provide a method to monitor the complete expression pattern of a cell in a single experiment (Southern, 2001). An array consists of a huge number of small DNA pieces that are each complementary to a certain gene (or rather transcript). When this DNA chip is incorporated with stained RNA or DNA, the probes bind to the spot on the array which is their complement. As the positions of each gene is known on a microarray, this enables the experimentalist to quantify the abundance of each gene transcript by analyzing the intensity of the stains. In practice two variants of microarrays are commonly used:

cDNA Arrays

cDNA arrays consist of pieces of DNA, that are complementary to the genes of interest (e.g. all 6000 yeast genes). They measure the relative RNA abundance of two probes and are therefore also referred to as *two channel arrays*. In an experiment the RNA of two cell types (e.g stressed and unstressed cells) is reverse transcribed to cDNA, which is labeled with a flurescent dye. In this step it is important to label the two different probes with two distinct dyes. Commonly, one probe is labeled with the green-flurescending Cy3, while the other probe is labeled with the red-flurescending dye Cy5. Hybridizing the mixture of the two probes with the array results in a competition of the two differently labeled probes for binding to the array. Therefore, a green spot on the array indicates higher transcript level in the first probe, while a red spot indicates the opposite. Consequently a yellow spot indicates a similar transcript level.

Oligonucleotide Arrays

Oligonucleotide arrays contain small oligonucleotide (≤ 25 base) strands, rather than larger copies as in the cDNA arrays. In general 11 to 16 copies of each gene are included in the array, which makes this type of array more specific, but less suitable for global analysis of whole genomes. Another difference to the cDNA arrays is, that only one probe is analyzed in one experiment, instead of comparing two expression patterns. The technical difference is that the cDNA derived from the cellular RNA, is again transcribed to cRNA, which then is hybridized to the array.

1.4.2 Analysis of polysomes

The activity at which mRNAs are translated is regulated both globally and specifically (Johannes et al., 1999; Zong et al., 1999; Kuhn et al., 2001; Mikulits et al., 2000; Brown et al., 2001). The underlying mechanisms are described in section 1.3.1. The translation state can be measured globally and for specific mRNAs. The methods how this is done are described in this section.

Global polysomal profiling

A method to determine the global translation state of a cell is to separate the differently loaded mRNAs by centrifugation, and to measure the abundance of RNA along this segregation by absorbance of ultraviolet (UV) light. RNA absorbs light with at a wavelength of 254 nm, and the absorbance of a solution containing RNA is proportional to the containing amount of RNA. More precisely, the absorption at a certain wave length A is the concentration C multiplied with way the light has to go through the solution I and an extinction coefficient ε ($A = \varepsilon CI$).

This method has been used for example in (Swaminathan et al., 2006; Ashe et al., 2000; Dickson, 1998). In the first step the cellular RNA, which is still being translated by ribosomes is extracted and separated by high speed sedimentation centrifugation. This method separates by density, thus the higher translated mRNAs are driven to the bottom of the centrifugation tube. In the next step fractions are collected from the separated solution by isotonic pumping, and changing the collecting bin at certain time intervals. These fractions contain the same mRNA with different numbers of bound ribosomes and can be used for the specific analysis described in the next paragraph. A global profile of the translation state of the cell can be gained by monitoring the absorbance at wavelength 254 nm during the isotonic pumping.

Figure 1.3 shows an example of how such a measurement of the absorbance looks like. The isotonic pumping starts from the top of the centrifuged solution, wherefore the highly translated mRNA pertains to the right side of the graph. The high absorbance at the beginning of the pumping is due to the absorbance of other solutes than RNA. After that, the graph shows peaks for the big and small ribosomal subunit, and thereupon a big peak for the mRNAs that are translated by one ribosome (monosomes). Behind the monosomes follow the different polysomes. Since the polysomes consisting of more than 10 ribosomes can not be distinguished

in this analysis, they are pooled together. Furthermore this method gives no estimation for the amount of mRNA that is not engaged in translation.

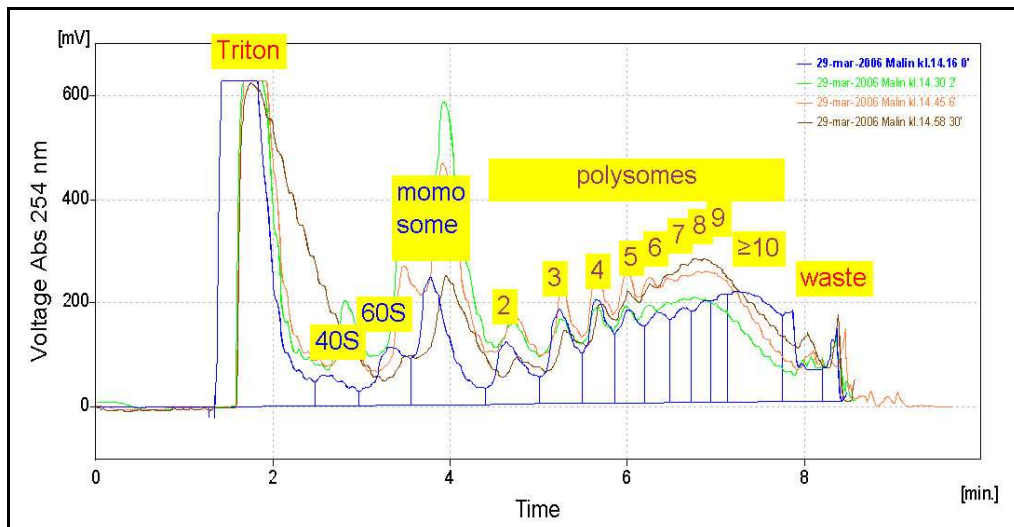


Figure 1.3: Example for a measurement of the global polysomal profile. Cellular RNA with the associated ribosomes has been separated by gradient centrifugation. The gradient has been monitored for it's RNA content by measuring the UV absorbance.

Specific polysomal profiling

In addition to the global analysis of the translation state, it is also possible to monitor the change in translation for single mRNAs. Two methods are available here, the first determines the abundance of certain mRNAs by northern blotting, and the second by DNA microarrays.

For the northern blotting method the RNA from the fractions collected during the isotonic pumping (typically up to 15) are run separately on agarose gels and probed by northern blotting. This gives a measurement for the abundance of individual mRNAs in the fractions. An idea how this looks like can be obtained from Figure 1.4 B, although in this case the shown procedure is not a northern blot but a simple RNA separation and subsequent staining. This method has been applied for example in (Kuhn et al., 2001; Swaminathan et al., 2006; Arava et al., 2003).

The second type of analysis is to use DNA microarrays to quantify the abundance of a huge number of mRNAs from one or more polysomal fractions. In general, a pool of polysomal fractions is compared to total mRNA by the use of two channel arrays. This gives an estimate of the translational activity of each single mRNA. This method has been applied in (Serikawa et al., 2003; Swaminathan et al., 2006; Mata et al., 2005). It can be extended by comparing multiple polysomal fractions to the total mRNA (MacKay et al., 2004). This approach is illustrated in Figure 1.4 C.

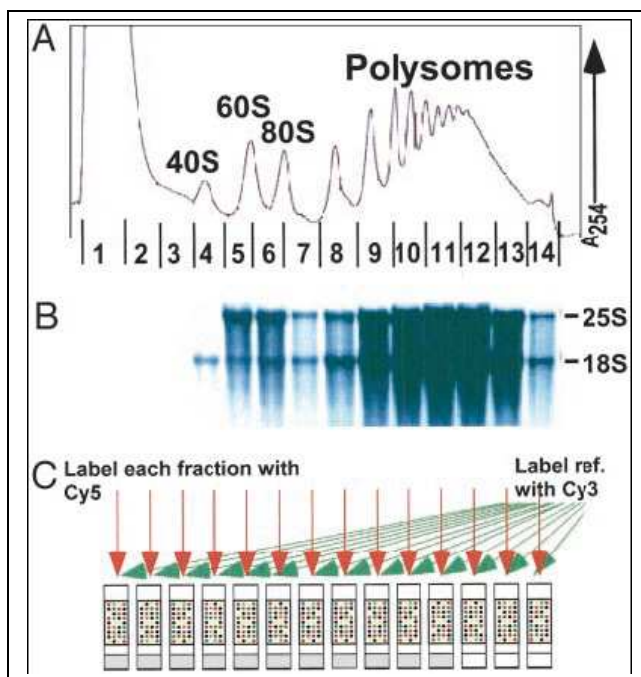


Figure 1.4: (A) Absorbance profile as already shown in figure 1.3. (B) Separating the RNA from each fraction by electrophoresis shows the different types of RNA in each fraction. (C) A specific polysomal profile for single mRNAs can be achieved by comparing the fractionated mRNA with the total mRNA on a microarray. Therefore the RNA from the fractions is reverse transcribed and labeled with Cy3, while the unfractionated RNA is reverse transcribed and labeled with Cy3. Figure taken from (Arava et al., 2003)

1.4.3 Gillespie algorithm for stochastic simulation

The Gillespie algorithm (Gillespie, 1977) is a method to simulate a chemical reaction system stochastically, which means that the algorithm chooses one possible way of the system, but does this according to the probability that the system would evolve in this way. A way is here defined as the number of all molecule numbers at each time point. When we consider a system of N metabolites with molecule numbers X_1, \dots, X_N at time point t that interact through M reactions, Gillespie's algorithm creates a time point $t + \tau$ at which the next reaction will occur, and states which reaction R_μ it will be. The important point is that the algorithm chooses these values according to the reaction probability density function of the system. The reaction probability density function $P(\tau, \mu)d\tau$ is the probability that, given the state (X_1, \dots, X_N) , the next reaction will occur in the infinitesimal time interval $(\tau, \tau + d\tau)$ and that it will be R_μ . This probability is the product of the probability that no reaction will happen in the interval $(0, \tau)$ times the probability that reaction R_μ will occur in the interval $(\tau, \tau + d\tau)$. The probability that there will be no reaction in the interval $(0, \tau)$ is

$$P_0(\tau) = e^{-\sum_{v=1}^M a_v \tau} \quad (1.5)$$

where

$$a_v = h_v c_v \quad (1.6)$$

is the product of the number of distinct molecular reactant combinations for reaction R_v h_v and the respective reaction constant c_v . The probability that a Reaction R_μ will occur in the interval $(t, t+dt)$ is just $a_\mu dt = h_\mu c_\mu dt$. Consequently, the reaction probability density function can be written as:

$$P(\tau, \mu) d\tau = a_\mu e^{-\sum_{v=1}^M a_v \tau} d\tau \quad (1.7)$$

Integration this equation over all possible reaction times gives the reaction probability distribution

$$P(R_\mu) = \frac{a_\mu}{\sum_{v=1}^M a_v} \quad (1.8)$$

and integration over all possible reactions leads to the probability distribution for the times τ

$$P(\tau) d\tau = \sum_{v=1}^M a_v \cdot e^{-\sum_{k=1}^M a_k \tau} d\tau \quad (1.9)$$

Therefore, the algorithm chooses for each step two unit random numbers r_1 and r_2 , and calculates from it τ and R_μ . From (1.9) and (1.8) it follows that choosing

$$\tau = (1/a_0) \ln(1/r_1) \quad (1.10)$$

where

$$a_0 = \sum_{v=1}^M a_v \quad (1.11)$$

and the reaction R_μ with μ being an integer for which

$$\sum_{v=1}^{\mu-1} a_v < r_2 a_0 \leq \sum_{v=1}^{\mu} a_v \quad (1.12)$$

holds true, gives the right probability density function for τ and R_μ .

The algorithm proceeds as follow:

0. Assign M reaction constants c_1, \dots, c_M and N molecule numbers X_1, \dots, X_N . Initialize time ($t = 0$) and reaction counter ($n = 0$)
1. Calculate a_i for $i = 1..M$ (1.6) and their sum a_0 (1.11).
2. Generate two unit random numbers r_1 and r_2 and calculate τ and μ according to (1.10) and (1.12)
3. Output X and t , update molecule numbers X_i for species participating in R_μ , set $t = t + \tau$ and if $t < t_{max}$ return to 1.

The running time can be improved by using a binary tree to compute a_0 and to find the a_i corresponding to r_1 (Gibson and Bruck, 2000).

1.4.4 Differential Evolution algorithm for optimization

Differential evolution (DE) (Storn and Price, 1997) is a heuristic to find the minimizing parameters for an arbitrary input function. The algorithm operates stochastically as the starting parameters are chosen randomly, and the search for the best parameter also involves throwing dices. The strategy is similar to the natural selection theory, wherefore DE borrows its terminology.

The aim is to minimize an objective function with a certain set of parameters (p_1, \dots, p_D) , for example the mean square difference of data points and a proposed function to generate these points. In the beginning NP parameter sets (vectors of length D) are chosen randomly. These NP vectors form the first generation, from which the succeeding generations evolve. The formation of the succeeding generation is done by randomly combining the preceding generation vectors. When a newly generated vector yields a better result than its predecessor, it replaces the predecessor, otherwise it is discarded. The generation of the new vector generation takes place in a two step process:

Mutation

Given the vectors of generation G $X_{1,G}, \dots, X_{NP,G}$ a new vector generation is created by choosing NP vectors V_i according to

$$v_{i,G+1} = x_{r_1,G} + F \cdot (x_{r_2,G} - x_{r_3,G}) \quad (1.13)$$

where r_1, r_2 and r_3 are random indices and F is a constant factor $\in [0, 2]$ that has to be specified by the user. F controls the amplification of the variation.

Crossover

In addition to the construction of parameter vectors as a random linear combination from preceding vectors, DE includes another stochastic process, as it mixes values from the preceding vectors with values from the newly generalized vectors to generate trial vectors. Therefore the user has to specify a crossover constant CR , which determines the rate at which the newly generated parameters are included in the trial vector. Exactly spoken the trial vector is formed according to

$$u_{j,i,G+1} = \begin{cases} v_{ji,G+1} & \text{if } (randb(j) \leq CR) \text{ or } j = rnbr(i) \\ x_{ji,G} & \text{if } (randb(j) > CR) \text{ and } j \neq rnbr(i) \end{cases} \quad (1.14)$$

$$j = 1, 2, \dots, D$$

whereas $randb(j)$ denotes a unit random number generator and $rnbr(i)$ a random index generator $1, \dots, D$. Because of its similarity to the genetic recombination this process is termed crossover.

Selection

To decide whether a trial vector $u_{i,G+1}$ replaces the target vector $x_{i,G}$ the outcomes of the objective function of the two vectors are compared, and the one with the smaller value is kept. This process is called selection.

Chapter 2

Model construction

2.1 Models

2.1.1 Single rate model

In a very simple approach to model the occupancy of mRNAs with ribosomes, one could suggest that ribosomes bind with a certain rate ka to the mRNA, and likewise dissociate with a certain rate kd . Thus the time it takes for the ribosome to translate the mRNA is not considered in this model. Another assumption of this model is that the number of bound ribosomes does not affect the binding rate of additional ribosomes. Since this model omits a lot of information about the involved processes, its biological meaning is questionable, but its a good starting point to look into the problems that arise when modeling ribosomal binding.

The reactions of the system can be written in the following way: Assuming that an mRNA can carry the maximum of N ribosomes, the reactions of the system can be written as



where M_i denotes an mRNA species with i bound ribosomes R and the index i runs from 0 to $N - 1$.

2.1.2 Multiple rate model

Because of steric hindrance the number of bound ribosomes should affect the binding rate of additional ribosomes, especially since ribosomes do not bind to an arbitrary location of the mRNA, but instead all bind to the 5' cap. To take this into account, the single rate model has been extended to make use of different binding rates for varying occupied mRNAs. The reactions considered in this model are equal to the single rate model, but the binding rates ka_i are distinct for each M_i . One way here is to assume a linear dependency between the binding rates $ka_i = ka \cdot \frac{1}{i+1}$ for $i = 0, \dots, N-1$. This implies a linear decrease of the binding rate, as more ribosomes bind. A different approach would be to consider each binding rate independently from the others, or to collect them in groups (e.g. M_0 to M_5 have the same binding rate, M_6 to M_{11} , and so on).

2.1.3 Bitstring model

The above described models have the shortcoming that the elongation process is not taken into account. This means that the time the ribosome is bound the mRNA, and the steric hindrance during the elongation process are not considered. To model this, one has to consider the position of each bound ribosome. An approach to do this, is to divide the mRNA in equable intervals and assume that these intervals are small enough, so that only one ribosome can bind to the interval. The representation of the mRNA translation state in this model is a binary vector of length K , where K is the maximal number of bound ribosomes. For example the vector (10000) denotes an mRNA with a single ribosome bound to the first position and the maximum of 5 bound ribosomes. When we consider every possible translation state of the mRNA as a separate species, we can write down the processes initiation, elongation, and termination as several reactions. To do this, it is most convenient to name each species after it's translation state vector, wherefore this model has the name bitstring model.

The processes initiation, elongation and termination inflate each to several reactions in this model.

1. Initiation

The initiation reaction is a reaction of the form



where each X can be either 1 or 0, wherefore this reaction stands actually for 2^{K-1} reactions.

2. Elongation

An elongation reaction can take place at each 10 pattern in the bitstring, producing a 01 pattern. Therefore we have to model $(K - 1) \cdot 2^{K-2}$ elongation reactions.

3. Termination

The termination reaction is formulated similar to the initiation:



where again each X can be 1 or 0

2.1.4 mRNA degradation and production

The above described models can be extended by adding a reaction that produces mRNA (transcription) or degrades it. Obviously, transcription should produce mRNA that is not occupied by ribosomes. But it is also reasonable to restrict the mRNA decay to not (or poorly) translated mRNAs, by assuming a competition between ribosomes and ribonucleases binding to the mRNA (Muhlrad et al., 1995; Jacobson and Peltz, 1996).

2.1.5 Degradation and production of ribosomes

As the number of ribosomes in a cell is probably nutrition-dependent (Warner, 1999), the models can be further extended by adding reactions for ribosome production and degradation. In this framework, only the degradation of free ribosomes is considered.

Chapter 3

Model analysis

3.1 Mathematical analysis

3.1.1 Single rate model

To characterize the dynamics of the single rate model, a mathematical analysis was done. But despite the rather simple structure of the model compared to the other ones, it was not possible to describe the steady state of the model exclusively by a mathematical expression. Notwithstanding the mathematical analysis revealed some notable traits of the model. Assuming mass action kinetics for the binding of a single ribosome to an mRNA, the differential equation system for the model reads:

$$\frac{d}{dt}M_0 = -ka \cdot M_0 \cdot R + kd \cdot M_1 \quad (3.1)$$

$$\frac{d}{dt}M_i = ka \cdot M_{i-1} \cdot R - kd \cdot M_i - ka \cdot M_i \cdot R + kd \cdot M_{i+1} \quad (3.2)$$

$$\frac{d}{dt}M_N = ka \cdot M_{N-1} \cdot R - kd \cdot M_N \quad (3.3)$$

$$\frac{d}{dt}R = \sum_{i=1}^N (-ka \cdot M_{i-1} \cdot R + kd \cdot M_i) \quad (3.4)$$

Whereas M_i denotes the concentration of mRNA with i ribosomes bound, R the concentration of unbound ribosomes, ka and kd the rate constants for binding and dissociation, and N the maximal number of ribosomes an mRNA can bind. Solving this system gives:

$$M_i = M_0 \cdot X^i \quad (3.5)$$

where $X = \frac{ka \cdot R}{kd}$
which leads to:

$$M_i = \frac{M_{tot} \cdot (x - 1)}{X^{N+1} - 1} \cdot X^i \quad (3.6)$$

where M_{tot} is the total mRNA concentration. (For proof see appendix)

First of all, it has to be mentioned that the given equations depend on the unbound steady state concentration of ribosomes rather than the total concentration, which makes it impossible to determine the steady state metabolite concentrations by just looking at the system parameters. Attempts to solve the system for the ribosome concentration failed, because the combination of formulae (3.4) and (3.5) results in a polynomial of rank N , which cannot be solved analytically for $N > 4$ (Abel, 1826). But some important conclusions can be drawn from the given formulas. The most interesting one is that the steady state concentrations of the different mRNA species always relate in an exponential manner ($M_1 = M_0 X^1$, $M_2 = M_0 X^2$ and so on). This implies that the concentrations of the different mRNA species in the model form a monotonic function. Another interesting property of the system is the dependence on the ratio of $ka \cdot R$ and kd , which is defined as X . When this is close to 1, the concentrations of the differently loaded mRNAs are close to each other. A ratio smaller than 1 leads to a distribution where the unbound mRNA has the highest concentration, whereas a ratio greater than 1 gives the inverse concentration pattern where the mRNA with the maximum number of bound ribosomes has the highest concentration (see Figure 3.1).

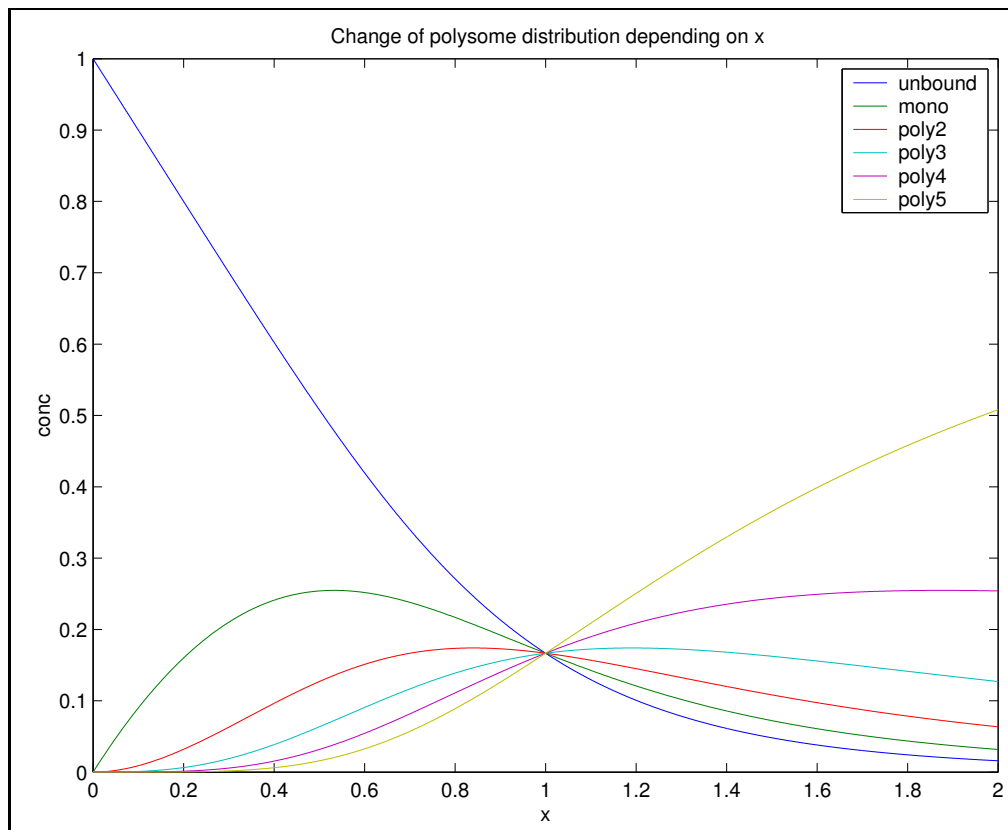


Figure 3.1: The influence of the ratio of $X = \frac{kaR}{kd}$ on the (relative) concentrations of the differently loaded mRNAs. The ordering by concentration gives an ascending ribosomal loading pattern for $X < 1$, and a descending one for $X > 1$.

For simulation of the model, this implies that when X crosses 1 during the simulation the

distribution pattern of the mRNAs gets inverted. This change may be due to altered values of ka or kd , which pertains to a regulation of the translation process, or it may be due to the degradation or production of ribosomes. Figure 3.2 gives an example, where the degradation of ribosomes leads to an inversion of the concentration pattern.



Figure 3.2: Simulation of the single rate model with ribosome degradation ($mRNA_i = \text{mRNA}$ with i ribosomes bound) . At time point 25 the value of $\frac{kaR}{kd} = X$ drops below 1 and the order of the different mRNA concentrations is inverted.

3.1.2 Multiple rate model

The multiple rate model differs from the single rate model only in having distinct initiation rates for the different translation states. Therefore, the derived formula for the concentration of each translation state looks rather similar to the one in the single rate model. The steady state concentration of mRNA with i ribosomes bound in is given by:

$$M_i = M_0 \cdot \prod_{j=0}^{i-1} ka_j \cdot \left(\frac{R}{kd} \right)^i \quad (3.7)$$

(For proof see appendix)

It is to mention that the concentration of each translation state depends on all the initiation rates of the lower transcribed mRNAs, which is not surprising since the ribosomes have to bind sequentially.

3.1.3 Bitstring model

The structure of the rate equations for the bitstring model is rather complicated and hence it was not possible to solve the rate equations analytically. Nevertheless, the derived rate equations are given here. In contrast to the single and multiple rate models, M_i denotes not the concentration of mRNA with i ribosomes bound but rather the concentration of the mRNA which translation state is represented by the binary string of i . For instance, M_2 denotes an mRNA with a single ribosome bound to the second last position ($M00010$ for $K = 5$). K denotes the maximal number of bound ribosomes, and $N = 2^K$ the number of distinct loading patterns for the mRNA. The rate equations read:

$$\frac{d}{dt}M_i = I(i) \cdot ka \cdot R \cdot M_{i-2^{K-1}} - T(i) \cdot kd \cdot M_i + \sum_{j=1}^{K-1} e \cdot (A(i, j) - B(i, j)) \quad (3.8)$$

$$\begin{aligned} \frac{d}{dt}R &= \sum_{i=1}^N (-ka \cdot M_i \cdot R \cdot I(i) + M_i \cdot kd \cdot T(i)) \\ &= \sum_{i=1}^{2^{K-1}} -ka \cdot M_i \cdot R + \sum_{i=1}^{2^{K-1}} kd \cdot M_{2i-1} \end{aligned} \quad (3.9)$$

where

$$N = 2^K \quad (3.10)$$

$$I(i) = \begin{cases} 1 & \text{if } \text{bin}(i)[1] = 1 \\ 0 & \text{else} \end{cases} \quad (3.11)$$

$$T(i) = \begin{cases} 1 & \text{if } \text{bin}(i)[K] = 1 \\ 0 & \text{else} \end{cases} \quad (3.12)$$

$$A(i, j) = \begin{cases} M_{i+2^{j+1}-2^j} & \text{if } \text{bin}(i)[j] = 0 \wedge \text{bin}(i)[j+1] = 1 \\ 0 & \text{else} \end{cases} \quad (3.13)$$

$$B(i, j) = \begin{cases} M_i & \text{if } \text{bin}(i)[j] = 1 \wedge \text{bin}(i)[j+1] = 0 \\ 0 & \text{else} \end{cases} \quad (3.14)$$

and $\text{bin}(i)[j]$ denotes the j th position of the binary representation of i

Since these equations are not too obvious, they need a bit of explanation. Formula (3.8) denotes the time derivation of the concentrations of the different translation states. This equation is formed by a term for the initiation ($I(i) \cdot ka \cdot R \cdot M_{i-2^{K-1}}$), a negative term for the termination ($-T(i) \cdot kd \cdot M_i$), and a sum over the different elongation reactions ($\sum_{j=1}^{K-1} e \cdot (A(i, j) - B(i, j))$). To understand these terms, one has to keep in mind that i actually denotes the decimal representation of a binary string. For example, M_4 represents the mRNA which translation state is described by the bitstring 00100 (for $K = 5$), that means an mRNA with a single ribosome bound to position 3. An mRNA species can only have been formed by an initiation reaction, if a ribosome is bound to the first position. This is indicated by $I(i)$, which

is 1 if the corresponding mRNA can have been formed by an initiation, and 0 if not. In addition, an mRNA species that is formed by initiation arises from the mRNA species with the same bitstring representation, with the difference that the first position is 0, whereas it is 1 in the formed species. Therefore, the mRNA species that forms mRNA species M_i by initiation is $M_{i-2^{K-1}}$. Thus, the contribution of initiation to the rate change of M_i is the product of the initiation rate ka , the ribosome concentration R , and the concentration of the uninitialized mRNA ($M_{i-2^{K-1}}$). $I(i)$ just indicates if $M_{i-2^{K-1}}$ is defined or not.

The Termination term in formula (3.8) can be explained in a similar way. An mRNA species can be degraded by termination, if a ribosome is bound to the last position. This is indicated by $T(i)$. Therefore, the contribution of termination is the product of the mRNA to be terminated (M_i), the indication if it can be terminated $T(i)$, and the termination rate kd .

The term for the elongation reactions is a bit more complicated. As explained in section 2.1.3, an elongation reaction is represented in the bitstring model by the change of a 10 pattern to a 01 pattern. Consequently, the degrading contribution of elongation can be described by a sum over all 10 pattern, and the forming contribution by a sum over all 01 patterns. Furthermore, a degradation corresponds to the considered mRNA (M_i), whereas a formation arises from the mRNA where the specific 01 pattern is a 10 pattern. The term $B(i, j)$ gives M_i if the considered position j in the mRNA M_i is a 10 pattern. That means the degradation contribution of elongation can be summed up by $-\sum_{j=1}^{K-1} e \cdot B(i, j)$, whereas e denotes the elongation rate. The function $A(i, j)$ gives the mRNA species from which M_i can be formed in the initiation reaction if M_i contains a 01 pattern at position i , and 0 otherwise. This mRNA species is $M_{i+2^j+1-2^j}$, since one is interested in the mRNA concentration where the 0 in the bitstring at position j is 1 and the 1 at position $j+1$ is 0. Combining these two effects one can write the elongation contribution as $\sum_{j=1}^{K-1} e \cdot (A(i, j) - B(i, j))$.

Equation (3.9) denotes the rate change of the ribosomes. This can be written as a sum over all mRNA species containing a negative term $-ka \cdot M_i \cdot R \cdot I(i)$ for the initiations and a positive term $M_i \cdot kd \cdot T(i)$ for the terminations. Since an initiation reaction can only take place if the first position is free, the initiation contribution can be rewritten by the sum over all mRNAs where the first position is 0 ($\sum_{i=1}^{2^{K-1}} -ka \cdot M_i \cdot R$). Likewise the termination requires a ribosome bound to the last position. Therefore, the termination contribution can be written as a sum over all uneven mRNA species ($\sum_{i=1}^{2^{k-1}} kd \cdot M_{2i-1}$).

3.2 Simulation analysis

The mathematical analysis revealed some properties of the single rate model, but it was not possible to derive a complete mathematical description for any of the presented models. For this reason, it seemed sensible to examine the behavior of the different models, by just simulating them with different parameters. The simulations were done with MATLAB (Matlab, 2005), which allows simulating any system that can be described by ordinary differential equations (ODEs). The process of simulating a system in MATLAB is exemplified in the appendix.

3.2.1 Single rate model

At first, a simulation of the single rate model with the maximum of $N = 10$ bound ribosomes was done. The parameters were $ka = 0.0015$, $kd = 1$ and the initial concentrations $M_0 = 10$, $M_i = 0$ and $R = 1500$. The concentrations can be interpreted as molecule numbers in this case, although the deterministic simulation admits also non discrete concentration values. The deterministic approach was favored to the more realistic stochastic, because the aim was to show the general system behavior, rather than to do a realistic simulation. Because the systems starts with concentrations far away from the steady state, and therefore may involve fast reactions, the stiff odesolver *ode15s* was used.

The simulation result is shown in Figure 3.3. As shown in the mathematical analysis, the steady state concentrations relate in an exponential manner to each other. In this case $X = \frac{kaR}{kd}$ is greater than 1, why M_{10} shows the highest concentration. Because of the exponential relation, the difference of M_{10} to the next mRNA (M_9) is greater than the difference of M_9 to its next (M_8), and so on.

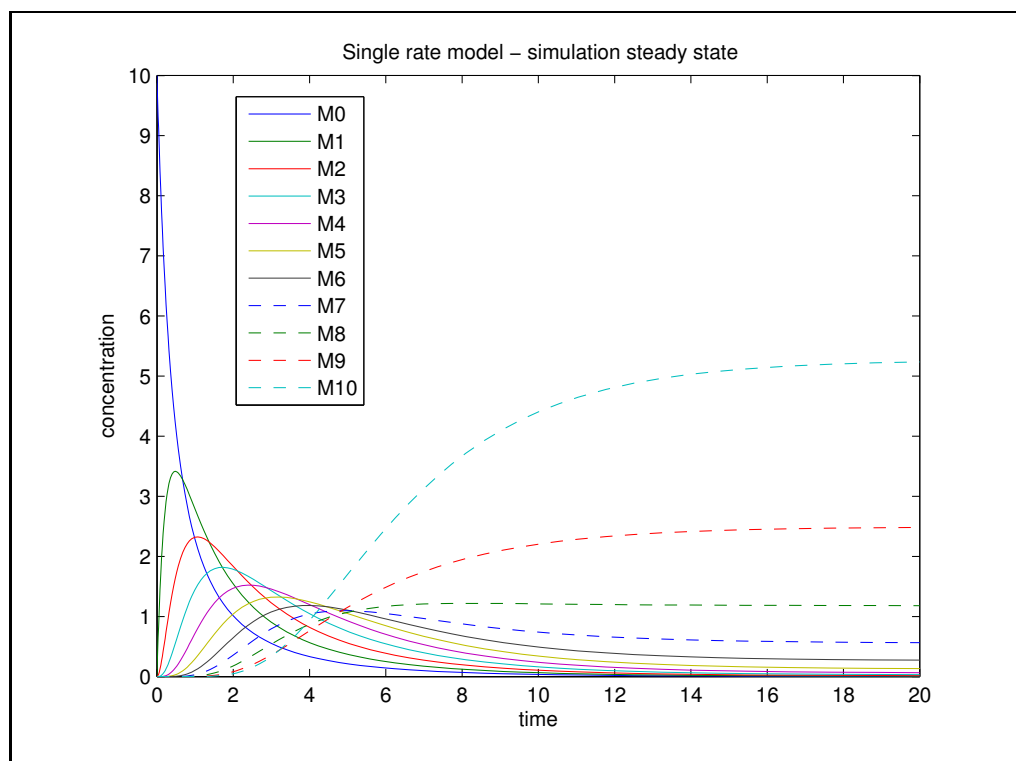


Figure 3.3: Simulation of single rate model

At time point 0 only the unbound mRNA has a concentration greater than 0. Therefore, the simulation could be interpreted as a rapid production of an mRNA species that was not present in the cell before. Though in living cells one would not expect that the production of a single mRNA species affects the number of unbound ribosomes notably (The ribosome concentration drops from 1500 to 1409 in this simulation). As one would expect, the concentrations of the

differently loaded mRNAs increases one after another, where the raise is the highest for the mRNAs increasing first. These are the mRNAs with few ribosomes bound. After this initial increase, the concentration drops again until the steady state concentration is reached. M_8 , M_9 and M_{10} do not show this descend, because on the one hand they have a high steady state concentration anyway, and on the other hand they reach their maximum not until the underlying mRNAs have leveled off. As already explained in the in the mathematical analysis, it is possible to invert the concentration pattern by either increasing kd or by decreasing ka (Simulation result not shown here).

3.2.2 Multiple rate model

The multiple rate model assumes a distinct initiation rate for each translation state of the mRNA. The most simple approach here, is to assume a linear dependency between the initiation rates. This means that each ka_i can be written as $ka_i = \frac{ka}{i+1}$ whereas i runs from 0 to $N - 1$. This model was simulated analog to the single rate model, but the general initiation rate ka was increased to 0.004. Figure 3.4 shows the simulation result.

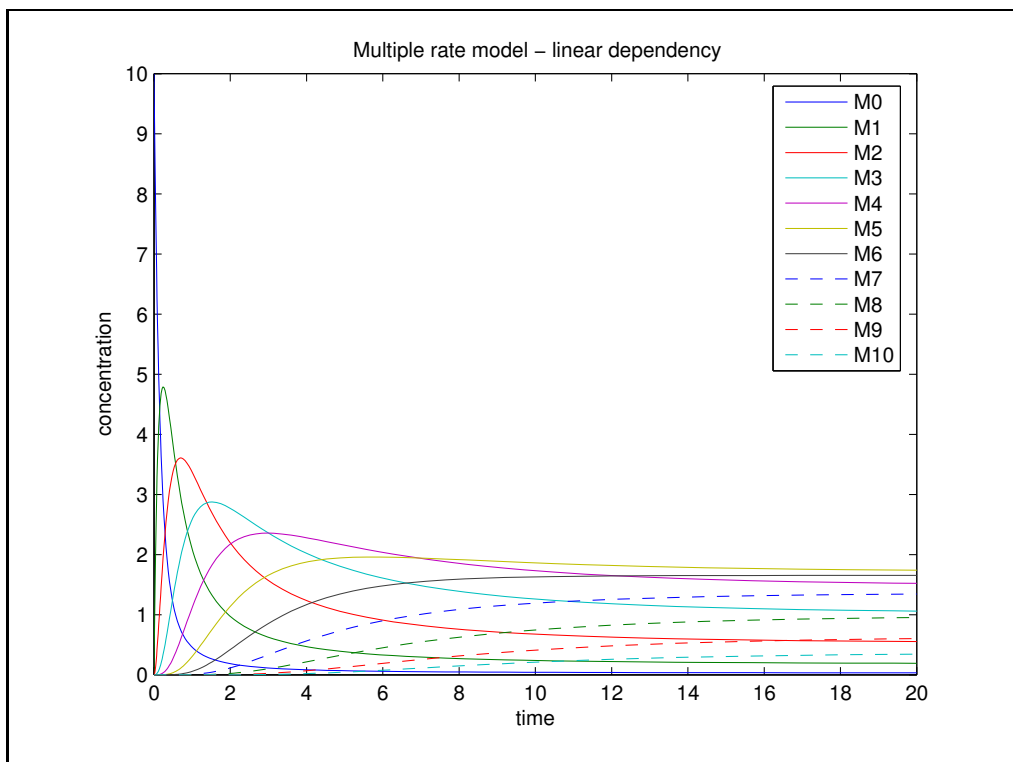


Figure 3.4: Simulation of the multiple rate model with linear dependency between the initiation rates $ka_i = \frac{ka}{i}$ for $i = 1..N$

The pattern of the temporal concentration increase of the differently loaded mRNAs is similar to the single rate model.

The interesting trait of the multiple rate model is that, in contrast to the single rate model, the concentrations of the differently loaded mRNAs do not form a monotonic function. Therefore, M_5 has the highest steady state concentration in this simulation. This distribution can not be reached with a single initiation rate, where the mRNA concentrations relate in a monotonic pattern ($M_i = M_0 \cdot X^i$). The simulation shows that up to M_5 the concentrations increase with the number of bound ribosomes, whereas it decreases for mRNAs with more than 5 bound ribosomes.

In addition to the simulation of the multiple rate model with linear dependent initiation rates, another simulation with arbitrary initiation rates was done. The parameters were here adjusted by hand, so that monosomes and highly translated mRNAs show a high concentration, while moderately translated mRNAs show a smaller concentration. This distribution was desired because it can not be reached by the single rate model, and in addition the ribosomal loading pattern is contrary to the simulation of the model with linear dependent initiation rates, where M_5 has the highest concentration. The simulation result is shown in Figure 3.5.

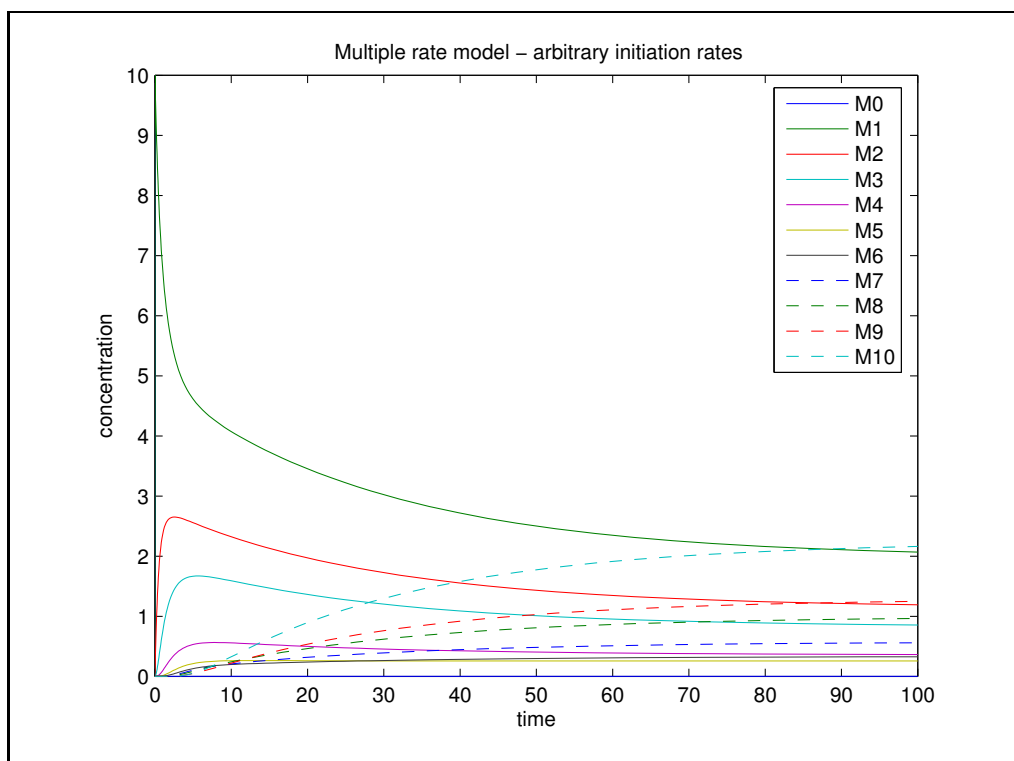


Figure 3.5: Simulation of the multiple rate model with arbitrary chosen initiation rates

As required, the highest steady state concentrations are made up by M_1 and M_{10} . Furthermore, the polysomes M_2 , M_3 , M_8 , and M_9 show also a relatively high concentration, while the concentration for the medium translated mRNAs and for the untranslated mRNA is low. This distribution of the polysomes is pictured in Figure 3.6.

The parameters that were used for this simulation are shown in Table 3.1.

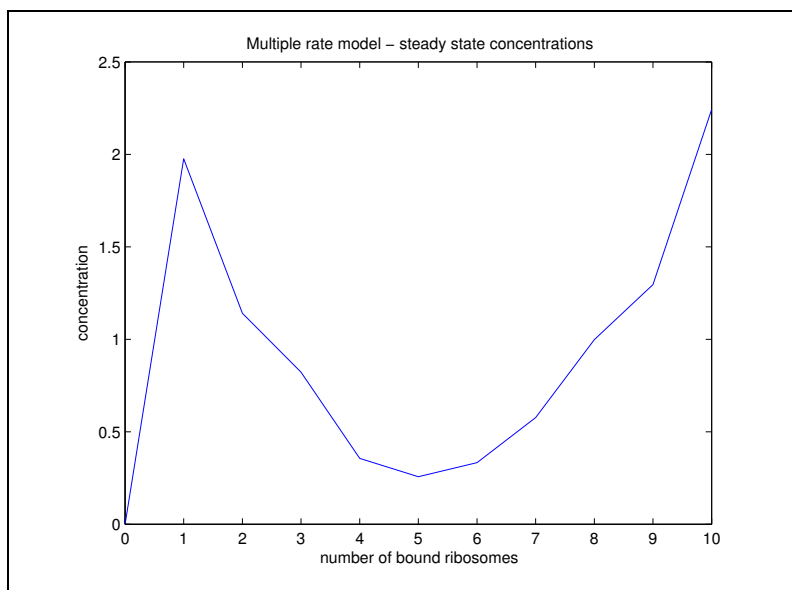


Figure 3.6: Steady state distribution of the polysomes in the simulation shown in Figure 3.5

ka_0	ka_1	ka_2	ka_3	ka_4	ka_5	ka_6	ka_7	ka_8	ka_9	kd
15	0.0004	0.0005	0.0003	0.0005	0.0009	0.0012	0.0012	0.0009	0.0012	1

Table 3.1: Parameters for simulation 3.5

The initial concentrations were the same as in the previous simulations. Interestingly the rate constant for the reaction directly forming M_1 , ka_1 is 4 orders of magnitude higher than the one for the reaction producing M_{10} , which shows a similar steady state concentration. This is because (i) the polysomal pattern depends not only on the distribution of the ka 's but also on the ratio of the total mRNA and ribosome concentration, and (ii) the concentration of each mRNA is not only determined by the rates directly acting on it but also on all the other rates for the preceding reactions (see Equation (3.7)). This is again reflected in the high value of ka_7 , while the proximate rates have a relative low value although the according concentrations are rather high.

3.2.3 Bitstring model

In contrast to the models examined so far, the bitstring model takes into account interactions between the ribosomes. The bitstring model has three parameters: the binding constant for the initiation ka , the rate at which ribosomes move forward one interval e , and the rate at which ribosomes dissociate when they reach the end of the open reading frame kd . Figure 3.7 shows a simulation result for $ka = 0.1$, $e = 1$, and $kd = 5$. The initial concentrations are again 10 for the untranslated, 0 for all other mRNAs, and 1500 for the ribosome concentration. It has to be noted that the different translation states are not made up by a single species in this

model, but rather by a sum over species. The monosomes for instance are actually the sum over 10 distinct species, because the single ribosome can bind to 10 positions. This makes the bitstring model computationally very demanding, as a model with K binding sites consists of 2^K species. Therefore, the temporal behavior of 1024 mRNA species had to be evaluated to calculate the shown results, as the model assumes a maximum of 10 bound ribosomes.

The most striking property of the bitstring model is that the polysomal distribution does not form a monotonic function as in the single rate model, although the initiation rate of the differently loaded mRNAs is determined by a single parameter. This behavior can be led back to the steric hindrance that is taken into account here, meaning that a new ribosome can not bind if there is still a ribosome bound to the initiation site. Also a ribosome can not move forward one interval, if there is already a ribosome bound to that interval. This mechanism makes very high translated mRNAs unlikely, as this would require that all ribosomes move forward synchronously.

The temporal behavior for the binding of ribosomes to the untranslated mRNA is, as one would expect, similar to the previous simulations. Remarkable is, that the raise of the monosomes is very fast compared to the polysomes. The explanation is again that, once a ribosome has bound to the first position, no other initiation can take place until the ribosome moves forward.

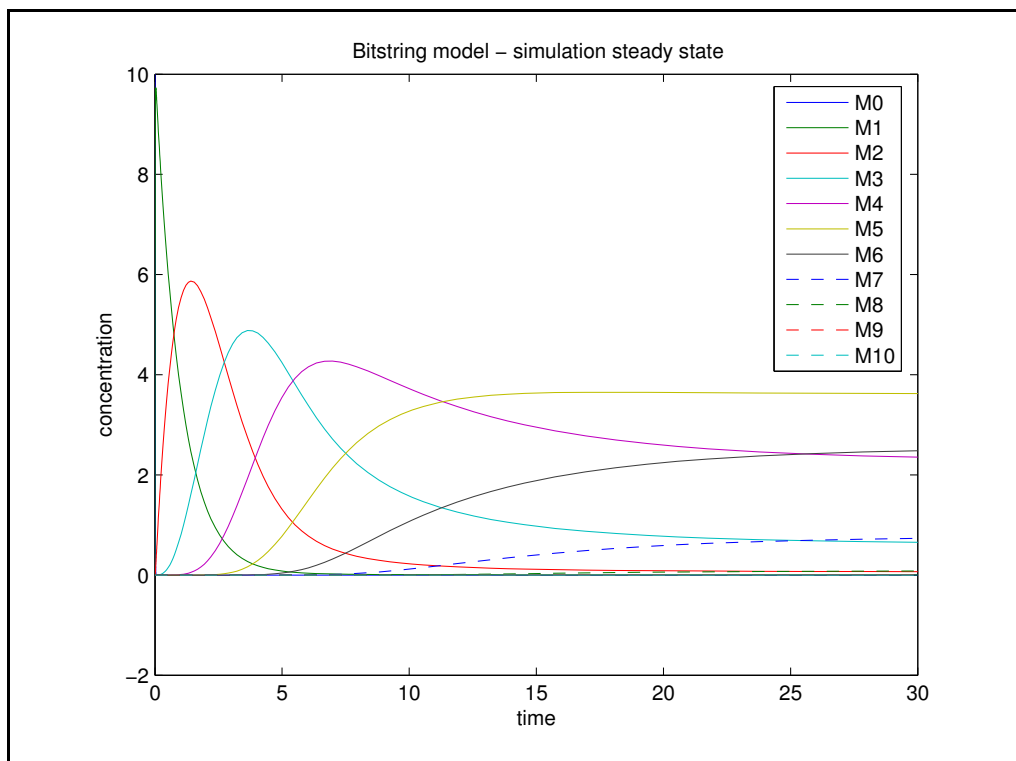


Figure 3.7: Simulation of the bitstring model with arbitrary parameters

In general it is believed that the initiation process is the rate limiting step in the translation

process (Jackson and Wickens, 1997; Lindahl and Hinnebusch, 1992; McCarthy and Kollmus, 1995). But one could assume a model where the termination is the rate limiting step. The bitstring model allows to examine consequences of such a model. Figure 3.8 shows a simulation where the initiation rate has been set to $kd = 0.5$ and the other values are kept from the first simulation. In this simulation the maximal translated mRNA has the highest steady state concentration. This is because the ribosome in the last position dissociates very slow, and thereby forms a bottleneck which hinders the other ribosomes from moving forward. In this constellation it is possible to achieve the maximal number of bound ribosomes, whereas this is very unfavorable under normal conditions, because it requires synchronously progressing ribosomes. As to expect, the binding of ribosomes right after simulation start is identical to the simulation where the initiation is the rate limiting step, with the difference that in this simulation also the higher translated mRNAs show a high amplitude.

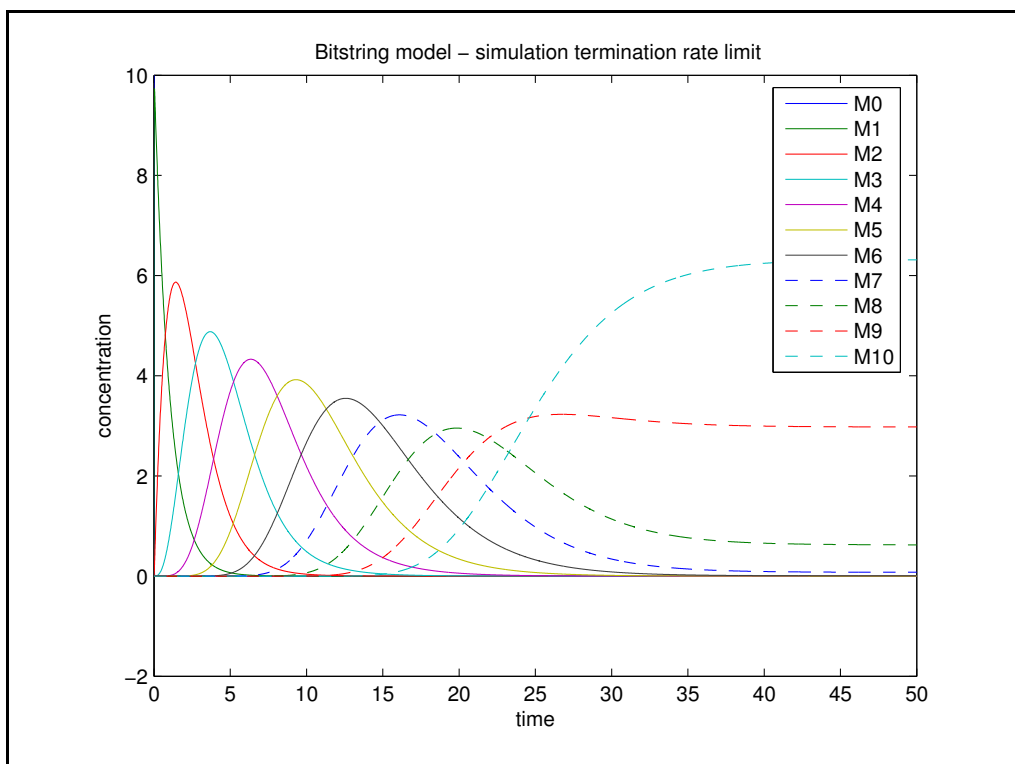


Figure 3.8: Simulation of the bitstring model with rate limiting termination

Chapter 4

Data fit

The aim of this work was to develop a model which is able to explain the temporal pattern of polysomal association of mRNAs that is found in yeast cells when subjected to osmotic stress. Therefore, the parameters for different models were adjusted in a way, so that they best describe the given data. The approach here was to fit the models to a steady state distribution of polysomes first, and to modify these models subsequently in a way such they can explain the temporal data.

4.1 Data

The data that the models were fit to are measurements of the polysomal association of the total mRNA in a cell. This data has been measured as explained in section 1.4.2. These measurements were done in the Department of Cell and Molecular Biology at the Lundberg Laboratory, Göteborg University, and were kindly provided for this thesis.

The data that has been used in this section are the measurements of the polysomal profiles in the yeast cells *Saccharomyces cerevisiae* in a 10 minute time window after osmotic shock. Figure 4.1 shows how the translation state of the cell changes after the osmotic shock. The values for the concentration of mRNA translated by ten or more ribosomes has been pooled in this data, and also there are no values for the concentration of untranslated mRNA. The value on the X-axis is not the absolute concentration of the mRNA, but indicates the extinction in the measurements and thereby the relative concentration.

It can be seen that under normal conditions most mRNA has bound 10 or more ribosomes. After the osmotic shock this distribution gets shifted, so that most mRNA is translated by monosomes. The time points 2 and 3 show an intermediate distribution, where both monosomes and polysomes have a relatively high concentration.

4.2 Used tools

Different tools have been tested to fit the models to the time points, and shall shortly be described at this point. Mathematically, a parameter fit is an optimization problem that

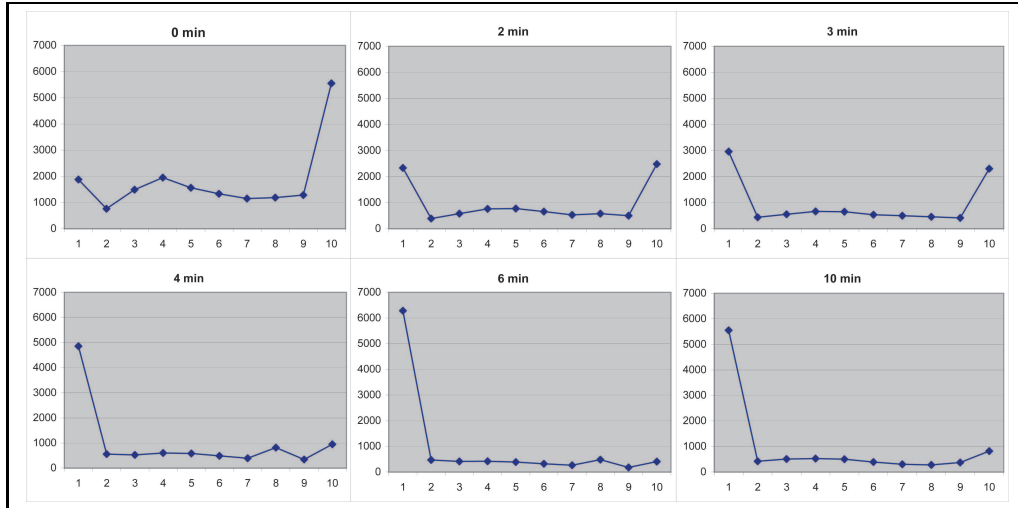


Figure 4.1: The change of the translation state after osmotic shock. The X-axis indicates the number of bound ribosomes, and the Y-axis the relative mRNA concentration. After osmotic shock the translation state drops from highly translated polysomes to prevailing monosomes.

minimizes the distances between certain data points and the according points in the model, by choosing the right parameters. This optimization problem can be tackled by either guessing the parameters in a smart way, or by directed search algorithms that evaluate the gradient of the system. In addition, it may be possible to fit the parameters by analytically solving the system, but this is only possible in few cases.

4.2.1 SBMLpet

SBMLpet (Zi and Klipp, 2006) is a parameter estimation tool that operates on files given in the Systems Biology Markup Language (Finney and Hucka, 2003) (SBML) format, which is a standard for the representation of reaction networks. Since all models developed in this thesis have been implemented in Dizzy (Ramsey et al., 2005), which offers an export to SBML, the program could have been used to fit all models. SBMLpet translates the SBML model to C source code, which can be compiled and runs therefore very fast. The program is able to handle normalized data, where the maximum value of each time point has been scaled to 1. SBMLpet works well for small SBML models, but importing the bitstring model with 10 binding sites failed because it was too large. Some models have been fitted with SBMLpet, but since the fits have been repeated using MATLAB these are favored for better comparability.

4.2.2 Berkeley Madonna

Berkeley Madonna (BM) ¹ is a commercial software to simulate systems that are given as differential equations. In this thesis only the free version of BM has been used, which does not

¹<http://berkeleymadonna.com>

allow to save models. There exist a Mathematica (Wolfram, 2003) SBML interface (Shapiro, 2004) which is able to export the BM format, but in this case it was easier to just reimplement the model in BM, since BM was only used with the multiple rate model which has relatively few differential equations.

A fit of the multiple rate model has been done for the different time points (as described for MATLAB in section 4.3.2). The fitting procedure of BM runs very fast, but no value is given for the goodness of the fit. To illustrate the goodness of the fit, plots of the data values against the predicted values of the fitted models for time points 0 and 4 are displayed in Figure 4.2. It can be seen that the fit for time point 0 is more or less acceptable, but the fit for time point 4 is not since the deviations are too large. Compared to the fit in 4.3.2, the results of the fits with BM are not convincing, and therefore are not shown here.

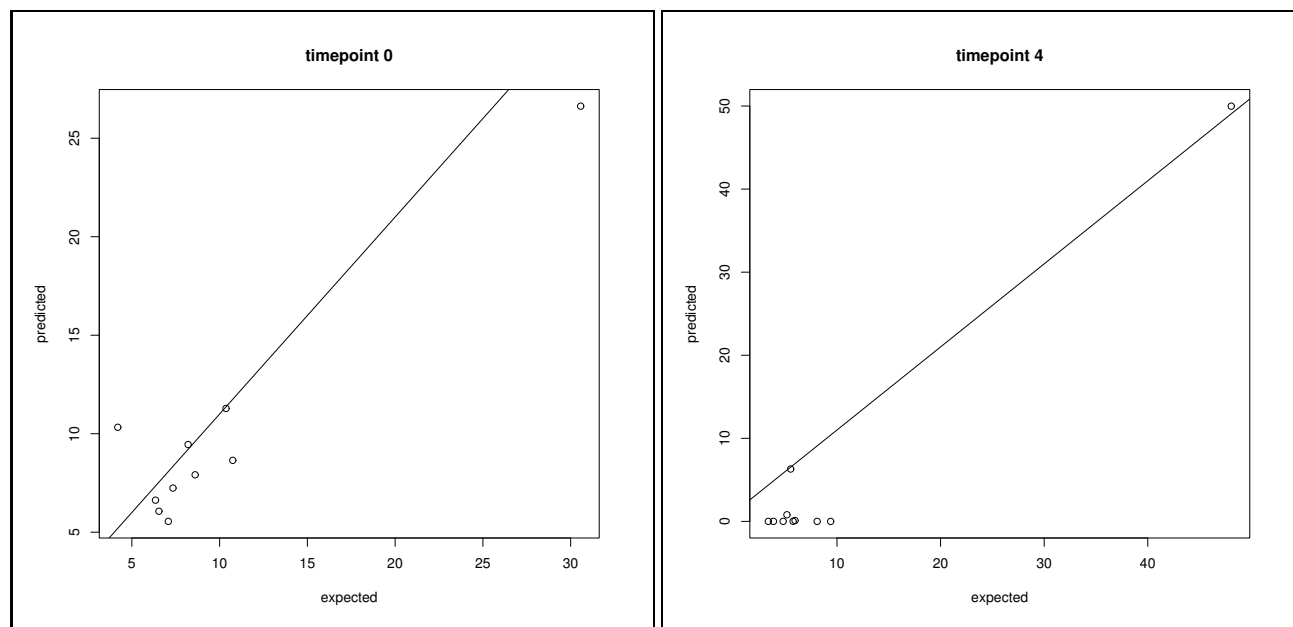


Figure 4.2: The values predicted by the multiple rate fitted with Berkeley Madonna mode have been plotted against the data values.

4.2.3 Matlab

Since MATLAB is able to simulate biochemical models (for example see appendix), it is also suitable for parameter estimation. For the parameter estimation with MATLAB the differential evolution (DE) algorithm was used (see 1.4.4). The MATLAB code for this algorithm can be downloaded from ². The process of parameter estimation in MATLAB is similar to simulating a system in MATLAB. One has to write an objective function, which determines for every parameter set the goodness of the fit. In this case, the objective function is called by the DE algorithm with a certain set of parameters. The objective function then simulates the system

²<http://www.icsi.berkeley.edu/~storn/code.html>

for the given parameters, determines the residual sum of squares (RSSQ) at a fixed time point, and returns this value to the DE function. This is done a lot of times during one parameter fit, and the best parameters are returned.

Parameter estimation with MATLAB gives the user by far more control over the procedure than SBMLpet or Berkeley Madonna, since optimization parameters can be specified, the model can be modified arbitrarily, and certain constraints can be included (This is also possible in SBMLpet). Because the estimation procedure is also very fast and underlying algorithm and procedure is known, MATLAB was used for the fits in this section.

4.3 Steady state fit

In the first step the polysomal distribution at different time points was considered as a steady state distribution. Of course the different time points do not correspond to a steady state, but this assumption was just accepted to compare the estimated parameter sets for these time points. This allowed to fit the models to the different time points independently, and to compare the resulting parameter distribution afterwards. The idea behind this was to derive a temporal model by looking at how the parameters for the different time points change in the same model.

To adjust the model to the data, at first the data was normalized, so that the sum over all concentrations equals 100. Since the measurements are relative measurements, the concentrations have no unit in this approach. The initial concentrations were chosen in a way that the total mRNA concentration is 110. The total concentration was chosen higher than it is in the normalized data, because the data does not include the untranslated mRNA. To fit the models to the concentration values of the different time points, the differential evolution (DE) algorithm (see introduction) was used with MATLAB. The DE algorithm requires an objective function, which determines for every parameter set the quality of the fit. In these cases the residual sum of squares (RSSQ) between the data and the predicted values at time point 60 were used. It is important to distinguish this simulation time point from the data time points, since we are considering each of the different time points as a steady state distribution. This time point was used, since it was assumed that 60 time steps are sufficient for the system to reach a stable distribution.

4.3.1 Single rate model

The single rate model has been fit to all six time points. The monotonic structure of the model implies that no satisfiable fit to a non monotonic polysomal distribution can be found. Time points 2 and 3 show such a monotonic distribution. Since the polysomes with 10 or more ribosomes bound have been pooled in the data, it was assumed in the model, that maximal 16 ribosomes can bind to one mRNA, and the concentrations were pooled together for polysomes consisting out of 10 or more ribosomes. The initial concentrations have been chosen to be $\frac{110}{17} \approx 6.47$ for each translation state (including untranslated mRNA).

time	ka	kd	ka/kd	$RSSQ$
0	0.267242	476.632364	5.6069e-04	36.06
2	0.000047	0.140580	3.3433e-04	178.73
3	0.000062	0.183990	3.3697e-04	353.12
4	0.100161	469.616672	2.1328e-04	701.09
6	0.163748	782.522937	2.0926e-04	1561.93
10	0.026837	127.616315	2.1029e-04	1103.90

Table 4.1: Parameters and residual sum of squares (RSSQ) of the fits of the single rate model to the different time points. In these fits the different time points have been considered as a steady state distribution, and the model has been fit to the single time point independently.

Table 4.1 shows the outcome of the fits: the parameters ka and kd , their ratio, and the RSSQ between the data and the prediction from the model. As expected the ratio of ka to kd decreases with the time, reflecting the redistribution from polysomes to monosomes after the osmotic shock. On the other hand, the RSSQ also increases significantly with the time. This can be explained (i) by the non monotonic distribution for time point 2 and 3 and (ii) by the pooling of the mRNAs with ≥ 10 ribosomes bound, which makes distributions with high monosomal concentrations unfavorable.

The results of a simulation of the fitted model with the estimated parameters are shown in Figures 4.3 and 4.4, where the data points are indicated as asterisks in the same color as the pertaining curve. It can be seen that, although the fit at time point 0 is not perfect (RSSQ=36), it is still much better than the fit at time point 10 (RSSQ=1104). The polysomal distribution at time point 0 is descending, except for the pooled M_{10} , which indicates that $\frac{kaR}{kd} = X$ is smaller than 1 (see section 3.1.1). Furthermore, all data points except the pooled M_{10} have a concentration close to 7, while the concentration for M_{10} is much higher. This is a distribution which complies with the developed model, because only M_{10} differs significantly from the other distributions.

At time point 10 the highest concentration in the data is made up by M_1 , while most other concentrations are very low. This distribution is very hard to reach with this model, as a high concentration for M_1 implies also a high concentration for M_2 and M_3 in the single rate model. In addition, the second highest concentration at time point 10 is made up by M_{10} , while the single rate model does not allow a non monotonic distribution of the different polysomes. Considering the very high RSSQ for most of the time points, it is very unlikely that the single rate model can explain the underlying biological processes in a satisfying way.

4.3.2 Multiple rate model

The multiple rate model has also been fit separately to the different time points. In contrast to the fit of the single rate model, the high translated polysomes were not pooled together in this model. This was not done because this would imply a very huge number of parameters,

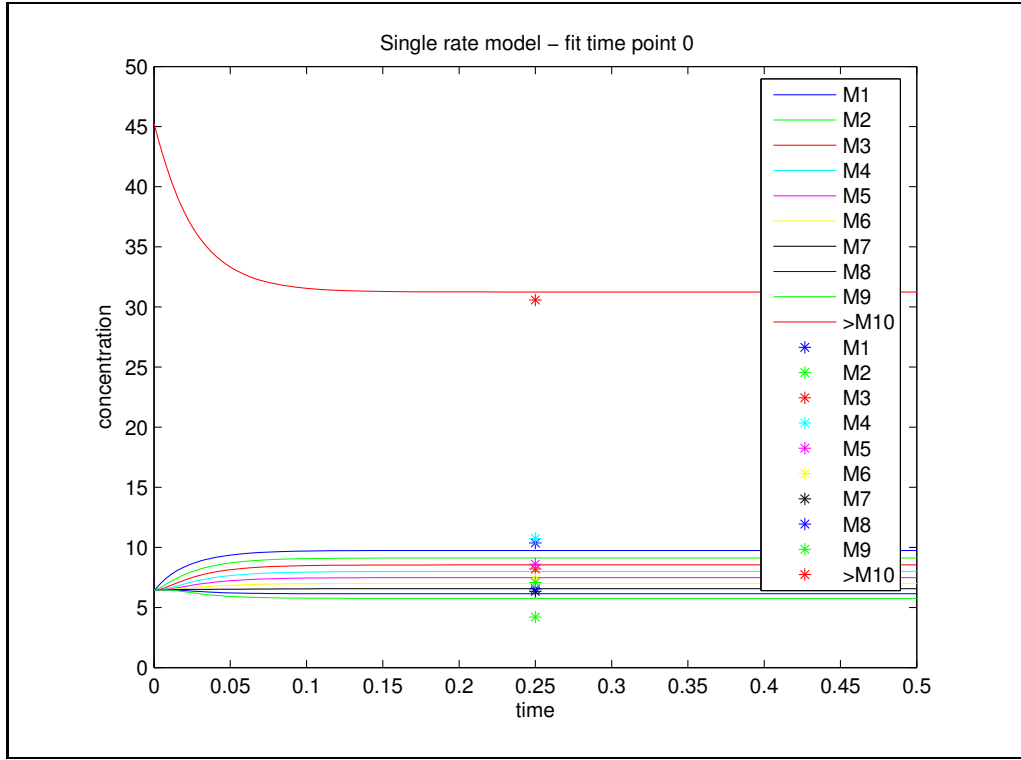


Figure 4.3: Simulation of the single rate model with the parameters estimated for time point 0. The data points are shown as asterisks in the same color as the pertaining curve.

since in the multiple rate model each translation state has its own initiation rate. The initial concentrations were 10 for each mRNA species, which gives a total mRNA concentration of 110, and again 1500 for the ribosomes. The result of the parameter estimation is shown in Table 4.2.

As to be seen, the model explains the data in an almost perfect way, since no RSSQ has a higher value than 1. Indeed this was to be expected, because a model with 11 parameters should be able to explain 10 data points. On the other hand, all the velocity constants are very high, which indicates very fast reactions. This is not very realistic, but results from the objective function that does not discriminate very high reaction constants. The parameters are also shown in a normalized way, where the highest value of each time point (the dissociation rate) has been rescaled to 1. These normalized values can be compared with each other, and make more sense in a biological way than the extremely high reaction constants derived from the DE algorithm. The differences in the errors between the normalized and unnormalized parameters may be due to rounding errors, since Equation (3.7) indicates that linear rescaling of all parameters should not affect the polysomal steady state distribution.

The initiation rates are much smaller than the dissociation rates in this fit, but this should not be interpreted because the ratio of the both depends on the concentration of total mRNA and ribosomes, which were chosen arbitrary in this case. Looking into the differences in the

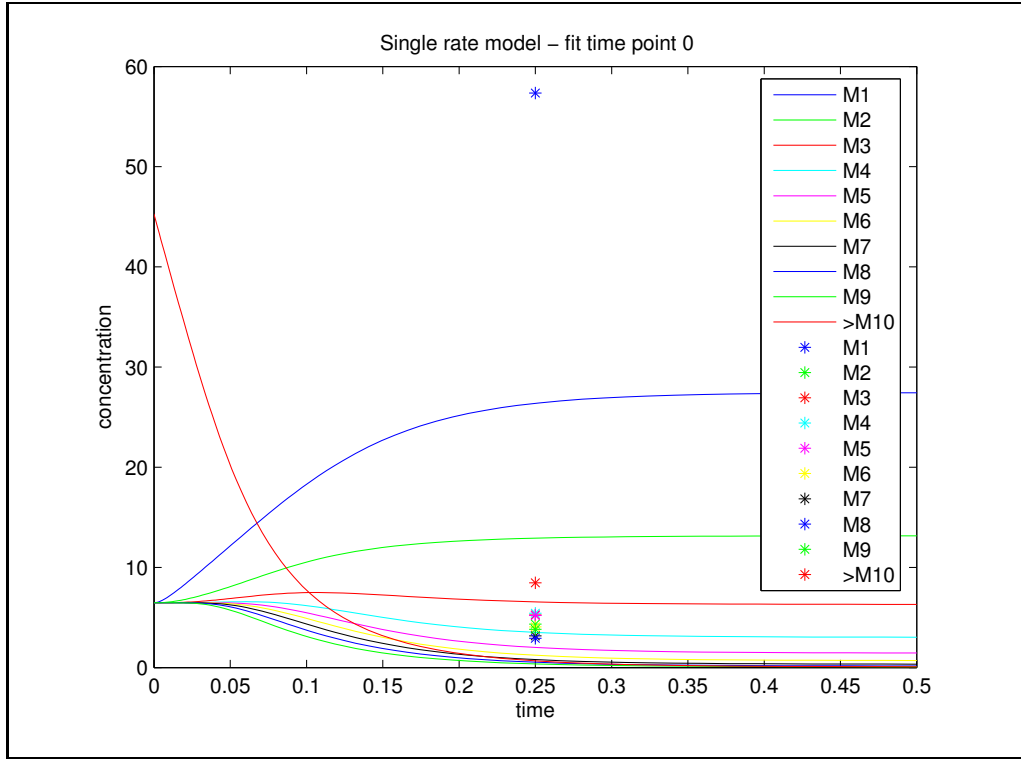


Figure 4.4: Simulation of the single rate model with the parameters estimated for time point 10.

normalized parameters for the different time points reveals that the initiation rates for the untranslated mRNA (M_0) raises about four fold from time point 0 to 10. In contrast, the initiation rate for M_9 drops to half of its initial value. This was to expect, since the distribution changes from highly translated polysomes to monosomes. Interestingly, the initiation value for M_1 , ka_1 also drops significantly, although the concentration of M_2 does not change notably over the different time points. This can be explained by the raising concentration of M_1 , which also determines the concentration of M_2 . To balance this, k_1 has to drop. The other initiation rates do not change notably over the different time points, as their corresponding concentrations also not changes.

4.3.3 Bitstring model

As mentioned beforehand, the bistring model is computationally very demanding. Because of this, a fit was only done for one time point, and even for this one fit the number of iterations was much lower than for the other fits. For instance, in the single rate model the shown fits are each based on 5000 to 20000 iterations per time point, whereas the shown data for the bitstring model is based on 150 iterations.

time	ka_0	ka_1	ka_2	ka_3	ka_4	ka_5	ka_6	ka_7	ka_8	ka_9	kd	$RSSQ$
0	1064	434	2083	1382	888	903	957	1047	1187	4637	1510438	0.1829
2	5010	344	3099	2752	2196	1795	1739	2175	1885	10289	3138069	0.1249
3	7359	347	2918	2580	2261	1911	2253	2158	1945	13003	3539761	0.3221
4	22168	538	3915	5151	4432	3623	3488	9550	1716	13215	7452302	0.1843
6	43668	528	5237	6891	5916	5540	5928	10938	2428	15481	11744738	0.2267
10	18778	271	3632	4005	3129	2737	2990	2716	4810	7477	5992164	0.5478
0n	0.0007	0.0003	0.0014	0.0009	0.0006	0.0006	0.0006	0.0007	0.0008	0.0031	1.0000	0.1788
2n	0.0016	0.0001	0.0010	0.0009	0.0007	0.0006	0.0006	0.0007	0.0006	0.0033	1.0000	0.1261
3n	0.0021	0.0001	0.0008	0.0007	0.0006	0.0005	0.0006	0.0006	0.0005	0.0037	1.0000	0.3036
4n	0.0030	0.0001	0.0005	0.0007	0.0006	0.0005	0.0005	0.0013	0.0002	0.0018	1.0000	0.3031
6n	0.0037	0.0000	0.0004	0.0006	0.0005	0.0005	0.0005	0.0009	0.0002	0.0013	1.0000	0.8952
10n	0.0031	0.0000	0.0006	0.0007	0.0005	0.0005	0.0005	0.0005	0.0008	0.0012	1.0000	0.5979

Table 4.2: Parameters and $RSSQ$ estimated for multiple rate model at different time points. Time points with appended n show the normalized parameters.

The maximum number of bound ribosomes was limited to 10 in this model, which already leads to 1024 mRNA species. Since the highly translated polysomes have been pooled in the data, it would be more realistic to set this number to a higher value but a value of 16, as chosen in the single rate model, would lead to 65536 species, where 1024 is already at the border of being computable in this context. The result of the fit to time point 0 is displayed in Table 4.3.

time	ka	e	kd	<i>RSSQ</i>
0	0.000539	40.481332	0.423811	400.573768

Table 4.3: Parameters for the bistring model fitted to time point 0.

The *RSSQ* value is 400, which indicates that the fit is rather bad. But, as already mentioned, this fit is based on only 150 iterations, since the time consumption to simulate this model is very high. In addition, it was not possible to pool the highly translated polysomes, as it was done in the data.

One conclusion that may be drawn from the estimated values is that the initiation rate is the rate limiting step in translation, as this rate has a significantly small value in this fit. In addition the elongation reaction is very fast in this model. A simulation of the bistring model with the estimated parameters is shown in Figure 4.5.

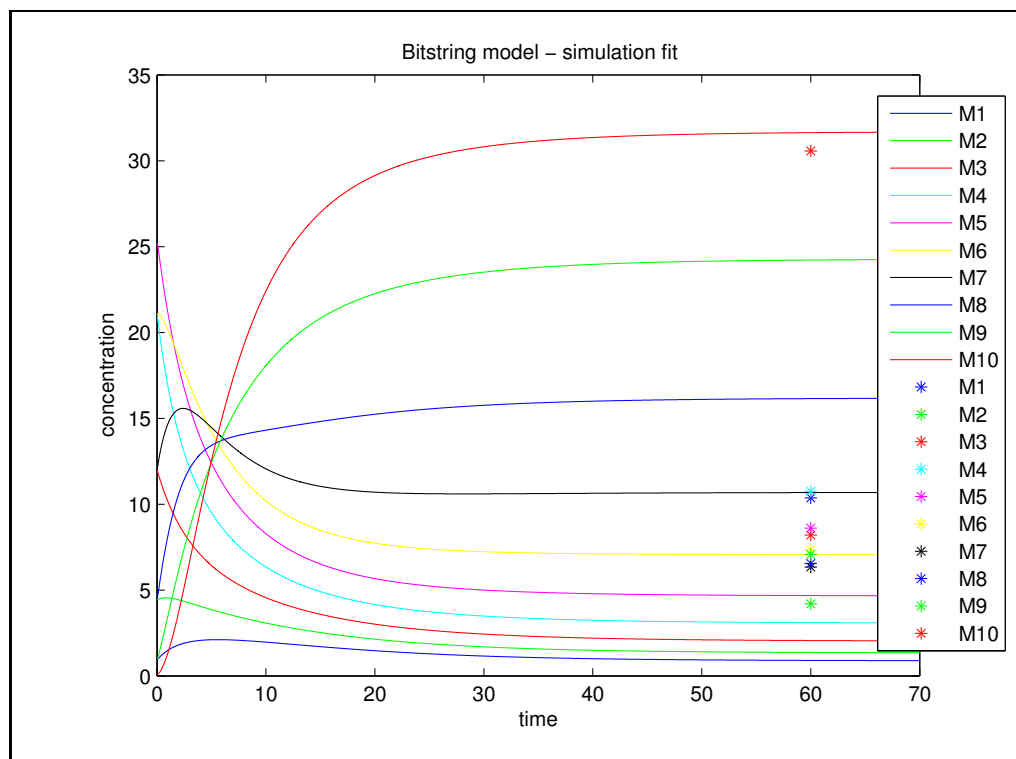


Figure 4.5: Simulation of the bistring model with the parameters derived from the fit to time point 0. Original data points are shown as asterisks.

4.4 Time course fit

The modes that have been fitted in the previous section were constructed to describe a steady state distribution of polysomes. Originating from these separated fits to the single time points, the aim was to develop a model that can explain the temporal behavior of the translation state after the osmotic shock. Because one could imagine different explanations for the translation state response after osmotic shock, these explanations were incorporated into the models, and the models were fit to the time course data. At the end, the different possible explanations were compared.

Two different approaches were chosen to fit the data: First, an additional reaction that may explain the change in the polysomal profile was added to the multiple rate model, whereas the parameters were kept from the previous fit to time point 0. In addition, a simplified multiple rate model with a lower number of parameters was fitted to the time course data. This second approach was not based on the previous steady state fits, but instead all parameters were guessed by the DE algorithm. The bitstring model was not used to derive a time course model because it was not possible to simulate it in an appropriate time, whereas the single rate model was not used because of its inability to explain the steady state data.

The additional reaction (or parameter change), that was supposed to explain the temporal data, was chosen to set in after the system has found a steady state. Therefore this reaction did not act before time point 50, wherefore time point 50 pertains to time point 0 in the data. The time scale was the same as in the data, so time point 52 pertains to time point 2 in the data, and so on. This means that the data fit was only done in the interval [50 60]. Since the time scale is in minutes in the data, this scale applies also to the models.

4.4.1 Multiple rate model

In the first approach, the multiple rate model was modified in a way that it may explain the data. The parameters and initial concentrations were taken from the previous steady state fit to time point 0, but in addition a reaction producing mRNA, or degrading ribosomes was included. Because only one reaction was added and the other parameters were taken from the preceding step, only one parameter had to be guessed by the estimation algorithm.

mRNA concentration change

The first model examined was the production of mRNA. Since the measured data gives no information about the total mRNA concentration, one could imagine that mRNA production leads to a redistribution of poly- and monosomes. A biological basis for this assumption is not given. Nevertheless, one would expect a shift from polysomes to monosomes in response to an mRNA production, since the available amount of ribosomes is shared between more mRNA. To examine the goodness of such a model explaining the time course data, it was implemented and fitted. The model used for this fit was the multiple rate model, with the parameters and initial concentrations from the fit to time point 0. In addition, a reaction producing mRNA

with a certain rate $k_{transcr}$, that sat in at time point 50 was included. Only the parameter $k_{transcr}$, was guessed by the DE algorithm.

The outcome of the DE algorithm is shown in Table 4.4. An RSSQ of 4681 indicates, that the model is not very good to explain the given data. Figure 4.6 shows a simulation result for the estimated parameter. The production of mRNA leads to a dramatic increase of monosomes (M_1), and interestingly to a light decrease in highly translated mRNA (M_{10}) concentration. The increase of M_1 can be explained (i) by the raising concentration of M_0 , from wich M_1 is formed, and (ii) by the fewer number of ribosomes, which leads to a redistribution from highly translated mRNA to lower translated ones. The decrease in the concentration of M_{10} is due to the fewer number of ribosomes. The restriction of the fit to the time interval [50 60] has the shortcoming that the estimated mRNA production is very high, leading to an exponential mRNA increase after time point 50. Therefore, it could make sense to restrict the mRNA production to the time interval [50 60].

$k_{transcr}$	RSSQ
0.426314	4681

Table 4.4: Parameters estimated for the time course fit of the multiple rate model with mRNA production outgoing from the steady state fit model.

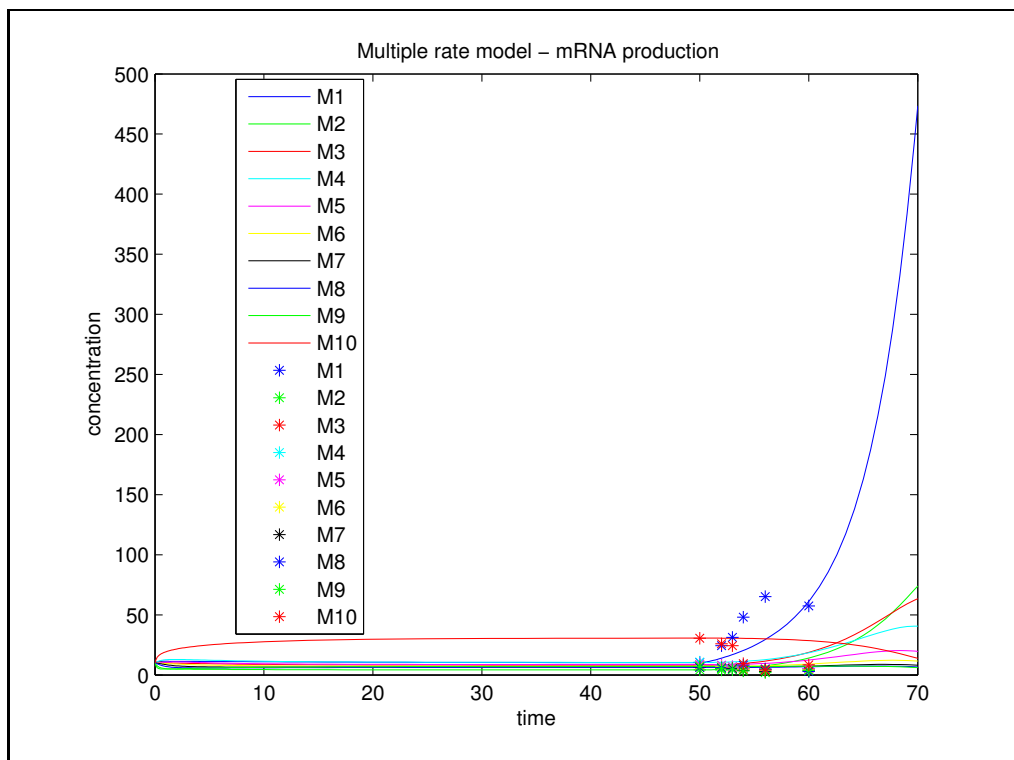


Figure 4.6: Simulation of the multiple rate model with mRNA production.

Ribosome concentration change

In the mathematical analysis it has been shown that a degradation of ribosomes can invert the concentration pattern in the single rate model. Therefore, one could expect that this rearrangement from polysomes to monosomes also takes place in the multiple rate model, if the ribosome concentration drops below a certain value. This approach has also been tested. The procedure was analog to the test of the mRNA production, with the difference that the reaction that produced mRNA was replaced by a reaction that degrades ribosomes with rate $R \cdot k_{degr}$.

The result of the fit is shown in Table 4.5 and a simulation with the estimated parameters is shown in Figure 4.7. The RSSQ of almost 7000 indicates that this model is not able to explain the data. As to be seen in the simulation, the degradation of ribosomes leads to a rapid concentration decrease of the highly translated mRNA M_{10} . In addition, the concentration of the monosomes M_1 shows a light increase, which is by far not as strong as in the data. Likewise a light increase in the beginning of the degradation can be seen for the less translated mRNAs M_2 and M_3 . The other polysomes show a decrease, since the available number of ribosomes gets smaller. Summing up it can be said that the increase of monosomes derived from the ribosome degradation is not strong enough to mimic the data. In contrast, the drop of highly translates polysomes (M_{10}) is similar in the model and in the data.

k_{degr}	RSSQ
0.23579	6927

Table 4.5: Parameters estimated for the time course fit of the multiple rate model with ribosome degradation outgoing from the steady state fit model.

4.4.2 Model with 3 initiation rates

In addition to the multiple rate model originating from the fit to time point 0, a hybrid of the single rate model and the multiple rate model was used, where the different translation states were split into three groups with different initiation rates. In this approach the untranslated mRNA M_0 , the mRNAs M_1 to M_{10} and the mRNAs M_{11} to M_{16} made each up one group. The mRNAs M_{10} to M_{16} were pooled together in the model, because also in the data the highly translated mRNAs had been pooled. The main difference to the previous fit is that in this case all model parameters are guessed, and no information from the previous fitted steady state is taken into account.

Initiation rate change

One could imagine that the drop from polysomes to monosomes after osmotic shock is due to a regulation of the initiation. Therefore a model was implemented, where the initiation rate drops linear with the time. This would correspond to a slow regulation of the initiation

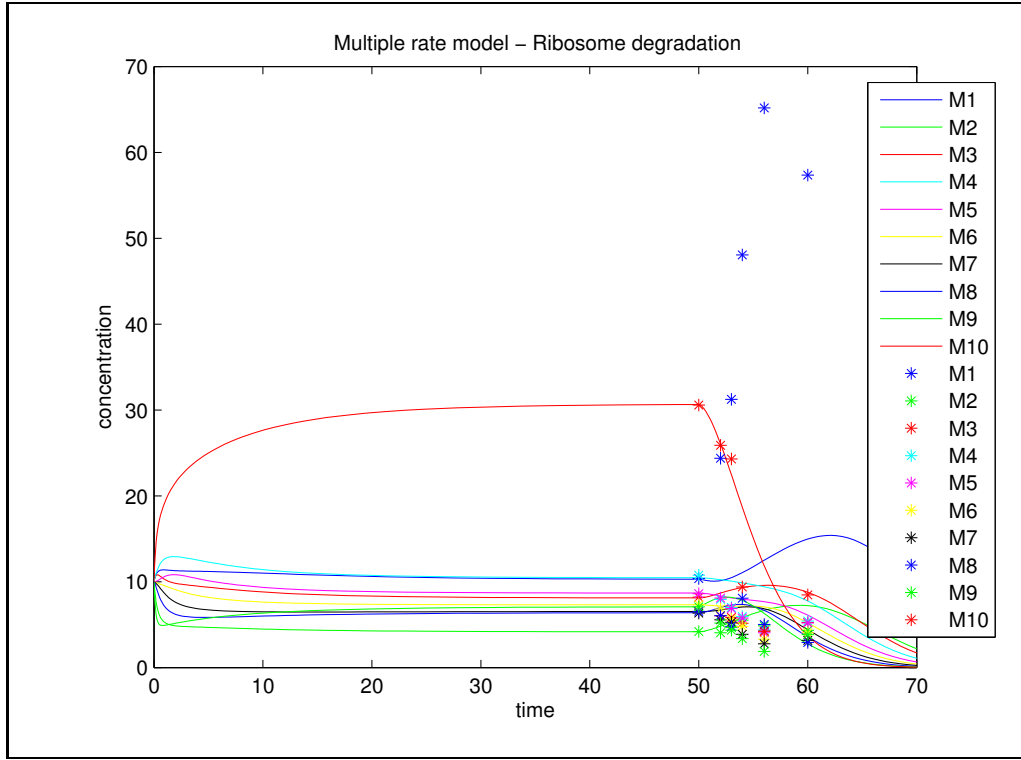


Figure 4.7: Simulation of the multiple rate model with ribosome degradation.

process. One could also assume a rapid regulation, what would correspond to a step function instead of a linear decrease. In this model the initiation rates after time point 50 are changed to $ka_{new} = ka_{old} \cdot \frac{c}{c+t}$ where t is the time in minutes and k is a constant, that has been guessed by the DE algorithm.

Table 4.6 shows the outcome of the parameter estimation. The high RSSQ indicates that the result is not really satisfying, although the result is better than in the steady state fits, that are based more parameters. But, in contrast to the fit outgoing from the steady state, all parameters have been fit in this approach, whereas the initiation and dissociation rates have been taken from the fit to time point 0 in the previous fit. This enables the DE algorithm to adjust the parameters in a way that they better correspond to the temporal data. Figure 4.8 shows a simulation of the fitted model. It can be seen, that the curves go in the right direction, although the data is not explained perfectly. A drawback of the used fit method is that it focuses exclusively on the interval $[50 \ 60]$, whereas other time points are not taken into account. In this case this leads to a model which shows a very high increase of M_1 even after time point 60. This results in an undesired high concentration of M_1 . In this case one could improve the model by limiting the regulation to the time interval $[50 \ 60]$, in which the estimation takes place.

The drop of the initiation rate from time point 50 on leads to a rapid decrease of the M_{10} concentration, which makes up the highest concentration before time point 50. Likewise the

ka_0	ka_{1-10}	ka_{11-16}	kd	c	$RSSQ$
0.210333	0.000605	0.000702	1.005655	0.593045	621.73

Table 4.6: Parameters estimated for the time course fit of the multiple rate model with initiation rate change.

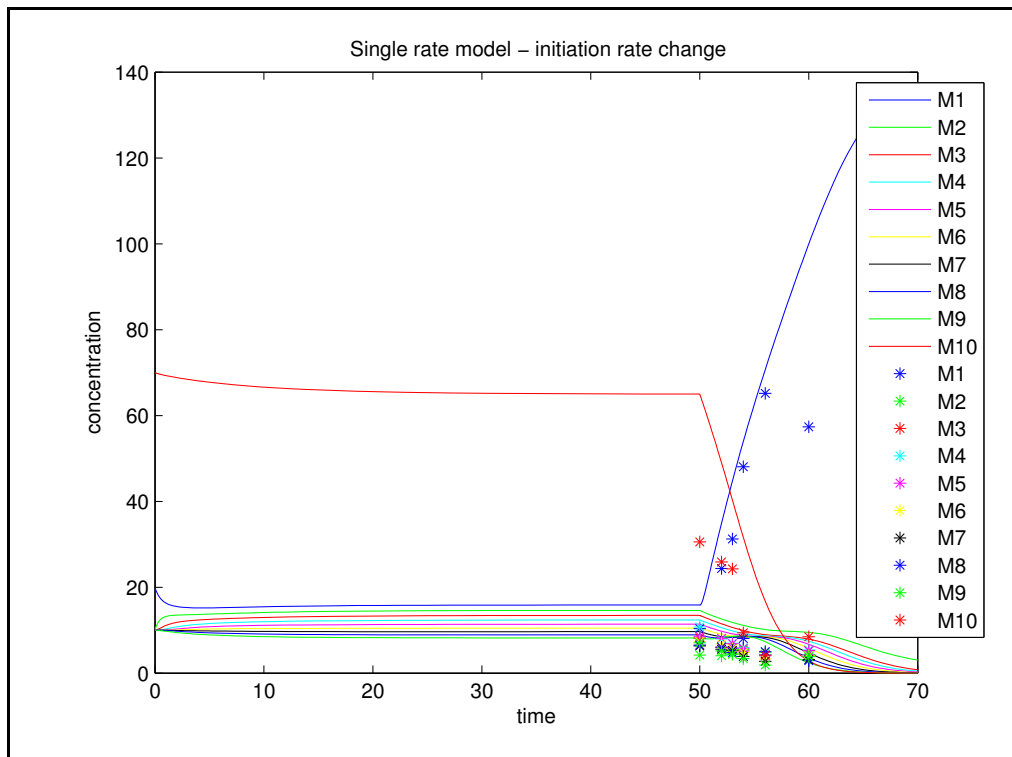


Figure 4.8: Simulation of the multiple rate model with initiation rate change from time point 50 on.

concentration of M_1 increases dramatically. This shift can also be seen in the data. A change in the model that can not be seen in the data is the drop of the concentrations of the mediately translated mRNAs. This happens because all initiation rates are changed in the same direction.

mRNA concentration change

The model, which includes mRNA production and that was tested for the multiple rate model, has also been tested for the model with three initiation rates. The procedure was analog to the fit for the initiation rate, with the difference that the initiation rate drop at time point 50 has been replaced by a reaction which produces mRNA with a certain rate k_{trancr} . This reaction produces mRNA with no ribosomes bound (M_0).

The estimated parameters are given in Table 4.7 and a plot of the simulated model is shown in Figure 4.9. An RSSQ of 2115 indicates that this fit is also not convincing. The simulation

indicates that M_1 shows a very fast increase, which is due to the production of M_0 . Likewise show the other few translated mRNAs also a slight increase, which is not supported by the data. The concentration of M_{10} shows a light decrease in the simulation, which is not affected by the mRNA production, setting in at time point 50. This decrease is due to the general small initiation rates in this fit, which lead to a very slowly adopting model.

ka_0	ka_{1-10}	ka_{11-16}	kd	$k_{transcr}$	$RSSQ$
0.001190	0.000690	0.016035	10.769169	28.042055	2115.22

Table 4.7: Parameters estimated for the time course fit of the multiple rate model with mRNA production.

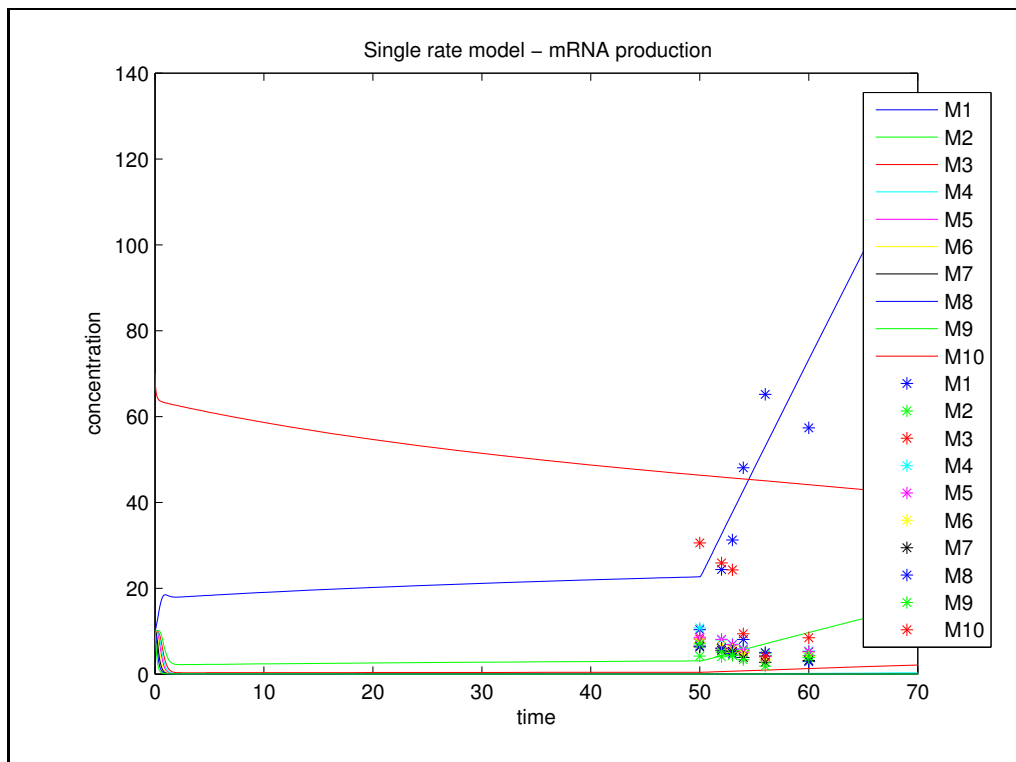


Figure 4.9: Simulation of the multiple rate model with mRNA production from time point 50 on.

Ribosome concentration change

Also the degradation of ribosomes was tested with the model comprising three initiation rates. The model with 3 initiation rates was extended in this case by a degradation reaction for the ribosomes, that sat in at time point 50. This reaction degrades ribosomes with a rate $R \cdot k_{degr}$, whereas R denotes the ribosome concentration. One would expect that the polysomal

distribution evolves in the direction of monosomes in response to ribosome degradation, since there are simply not enough ribosomes.

The result is shown in Table 4.8 and Figure 4.10. It can be seen that this fit has gone badly wrong, since the reactions are so slow that the system does not reach a stable distribution before the simulation ends. In addition, no appreciable change can be noticed at time point 50, where the degradation of ribosomes sets in. An explanation for this could be that the fitting procedure went wrong for some reason. For instance, the starting intervals for the parameters may have been chosen inappropriately. Because also the fit of the multiple rate model outgoing from the steady state distribution with included ribosome degradation showed a high RSSQ, it may be that the model just can not describe the data.

ka_0	ka_{1-10}	ka_{11-16}	kd	k_degr	RSSQ
0.000160	0.000000	0.000008	0.070577	0.000425	2551.752858

Table 4.8: Parameters estimated for the time course fit of the multiple rate model with ribosome degradation.

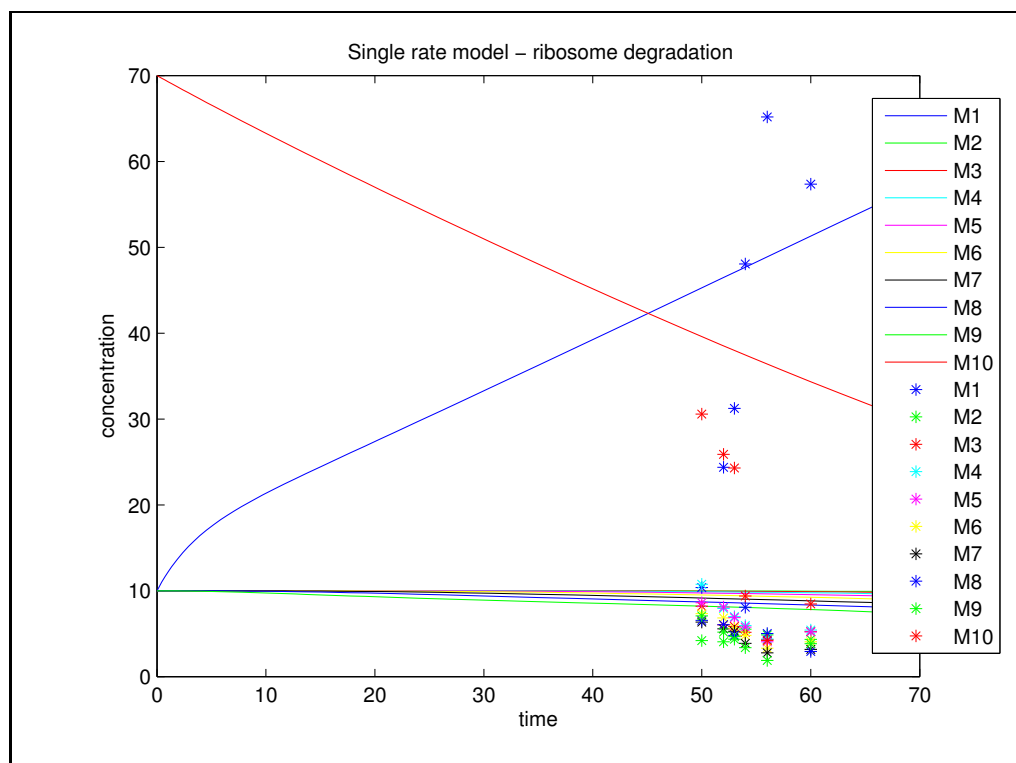


Figure 4.10: Simulation of the multiple rate model with ribosome degradation from time point 50 on.

Chapter 5

Results

5.1 Comparison

In this work, different models have been developed and prospected with regard to different processes explaining the change in polysomal profiles, that is found when yeast cells are subjected to osmotic stress. At this point, the different models, and the different probed processes shall be compared for their quality to explain the given data.

5.1.1 Models

Three models have been examined: (i) the single rate model, where the initiation rate does not depend on the number of bound ribosomes, (ii) the multiple rate model, where this is adverse, and (iii) the bitstring model, that takes into account the position of each ribosome on the mRNA.

Single rate model

The single rate model has a fairly simple structure, and is therefore only able to describe a monotonic pattern of the ribosomal association. This means that it is not able to form a distribution where both monosomes and highly translated polysomes have a high concentration, while mildly translated polysomes have a low concentration. For this reason the single rate model has not been used to construct a temporal model. The simple structure of this model has the advantage that at least some conclusions can be drawn from a mathematical analysis (e.g. monotonic structure, turning point). Though a complete mathematical description, for instance to fit the model analytically to data points, could not be derived.

Multiple rate model

The multiple rate model is an extension of the single rate model, where every translation state of the mRNA has its own rate for binding to a ribosome. This leads to a model with a lot of parameters, and it is questionable if this assumption is meaningful in a biological context.

Nevertheless, the multiple rate model is able to mimic the distributions of the measurements at the different time points in an almost perfect manner. Because of the enormous number of parameters, this had to be expected.

Two modifications of this model outgoing from the fit to the data at time point 0 were not able to mimic the temporal polysomal profile after the osmotic shock. This may be reducible, either to an inability of the model or of the examined processes to describe the data. An answer to this question would require a deeper analysis of the model and the processes.

In addition to the fit outgoing from a steady state distribution, a simplified version of the multiple rate model has been fit to the time course data, where all parameters have been estimated. In this simplified model the different translation states of the mRNAs were divided into three groups. Compared to the fit outgoing from the steady state distribution, this approach gives a better result, although it is still not satisfying. The explanation for this may be that all parameters are guessed in this approach, whereas in the first approach a fixed distribution was modified by a single influence.

Bitstring model

The bitstring model is the most complicated of the presented, since it simulates the binding position of each single ribosome to the mRNA. Because of this precision the model is very complex, and therefore could not be solved analytically. In addition, this complexity makes the model computationally very demanding to simulate. Therefore, it was not possible to fit this model to time courses, and also the fit to a steady state distribution was only possible in a limited way. This fit to a steady state distribution led to an inferior fit compared to the other models. But since the number of iterations of the estimation algorithm was much smaller in this case, the results are not comparable. The bitstring model is not restricted to a monotonic loading pattern as the single rate model, although all translation states have the same initiation rate in this model (not considering the states where a ribosome occupies the initiation site).

5.1.2 Processes

Different processes have been tested in this work that could explain the temporal change in the polysomal profile in response to osmotic stress. They have been incorporated into the multiple rate model and fitted to the time course data. The ability of the different processes to describe the data is compared in this section.

mRNA production

A process that might explain the polysomal profile change after osmotic shock would be an increase in the mRNA concentration. From the biological point of view this assumption is doubtful, since the mRNA level is believed to decrease after osmotic shock (Hohmann, 2002). Nevertheless, this assumption has been tested by implementing it into the multiple rate model, and fitting this model to the data. The mRNA production hypothesis was tested outgoing from

a steady state distribution, as well as by fitting all model parameters. In both cases the result was not satisfying, since the mRNA production can explain the increase of the monosomes but not the decrease of the highly translated polysomes. In addition, the mRNA concentration increased dramatically in the fitted model, which is not possible in such an extent in the reality.

Ribosome degradation

The second model that has been tested was a degradation of ribosomes. In the model outgoing from the steady state fit this could explain the drop of highly translated polysomes, but not the increase in monosomes. In the model where all parameters have been fit, this hypothesis led to a completely wrong model. This may be either because the model can not explain the data, or because the method to fit the data was inadequate. An improvement of the fit method would be to require the model to find a steady state before fitting the parameters, since the simulation in Figure 4.8 shows that this was not the case in this parameter fit.

Initiation rate change

A process that has only been examined outgoing from the model with three initiation rates was a drop in the initiation rate during the simulation. This corresponds to a regulation in the translation initiation process, which has been shown to exist (Kimball, 2001). In fact, this initiation rate change leads to a better result than the other analyzed processes. The initiation rate drop leads to a redistribution, where the concentration of highly translated polysomes drops and the concentration of monosomes increases. On the other hand, the concentration of mediate translated mRNAs drops as well, which is not supported by the data.

5.2 Validation

In addition to global translation state data, array data about the translation state of single genes was available. This data has been kindly provided by the Department of Cell and Molecular Biology at the Lundberg Laboratory, Göteborg University. In this data the polysomal and total mRNA of cells that have been subjected to osmotic stress were measured with DNA microarrays. Precisely spoken, the polysomal and total mRNA of stressed cells have been compared to total mRNA of unstressed cells. This was done by two channel arrays (see section 1.4.1). A more detailed analysis of this data was not part of this work, but some results are displayed and compared to a simulation result. Figure 5.1 shows three different clusters of a hierarchical clustering of the delta PAFs derived from the array analysis. PAF stand for polysomal association factor, and denotes the ratio of polysomal to total abundance of a certain mRNA species. The ratio of the PAF at two time points is called delta PAF. This delta PAF is shown in Figure 5.1 in a illustrated and quantified way for three differently regulated mRNA clusters. Because the delta PAFs are all compared to time point 0, the first value has always a value of 1, since it is compared to itself. The values are displayed in dual logarithmic scale, thus a value of 2 denotes a upregulation of factor 2 compared to time point 0.

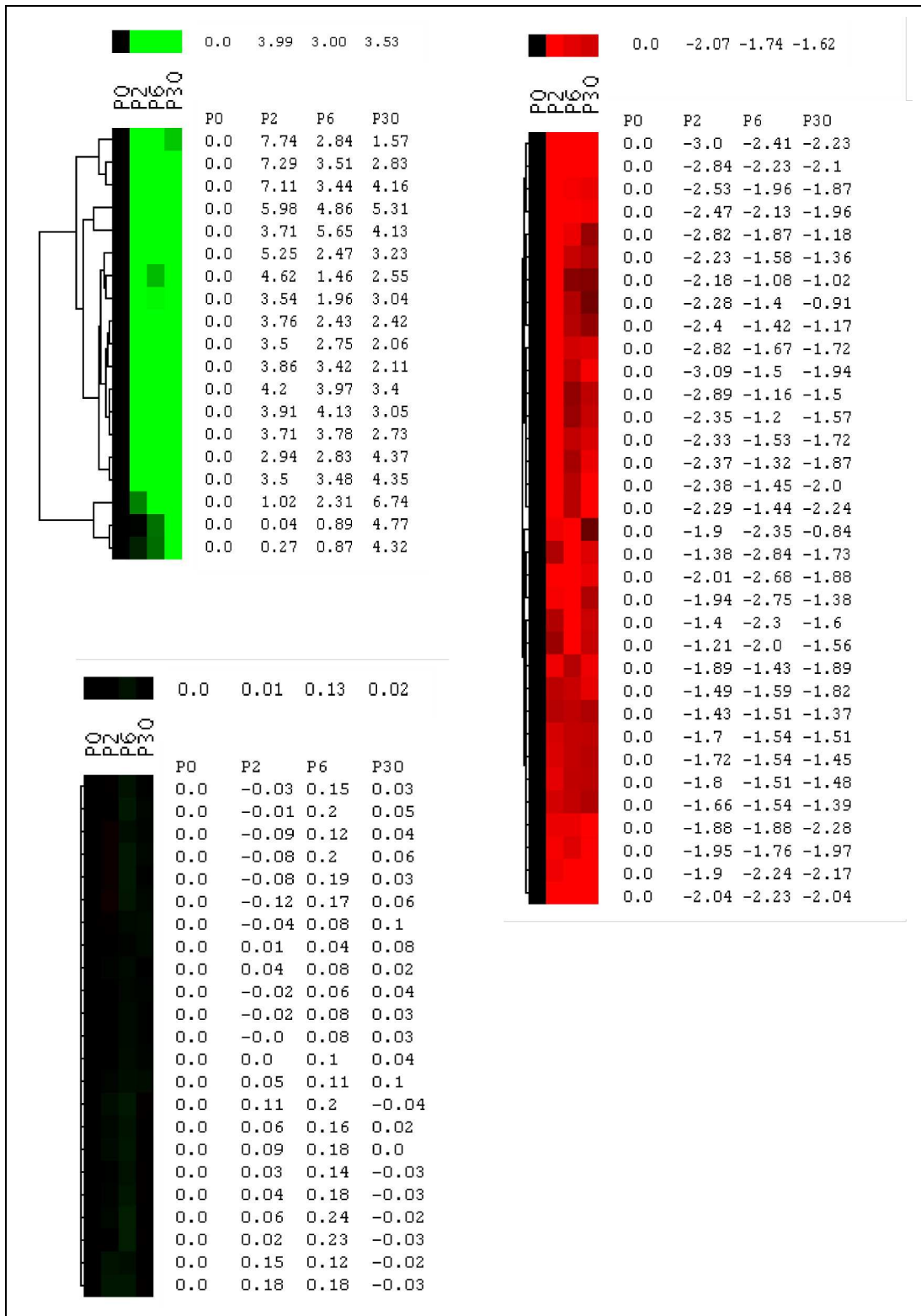


Figure 5.1: Change of the difference of the polysomal association factor to time point 0 (delta PAF) in response to osmotic shock for different mRNAs. Green: mRNAs that are upregulated in their translational activity. Red: mRNAs that are downregulated. Black: mRNAs that do not change their translation state in response to osmotic stress.

Three different clusters are shown in the figure: (i) a cluster of mRNAs that have been upregulated (green), (ii) a cluster of mRNAs that have been downregulated (red), and (iii) a cluster of mRNAs which polysomal profile did not change in response to osmotic stress (black). The names of the genes are not shown, since they are not evaluated at this point.

In this section, the bitstring model with the maximum of number of 5 bound ribosomes has been simulated stochastically. This model includes three different types of mRNA, an upregulated one, a downregulated one and a not regulated one. These mRNA classes differed in the model only in their initiation rate. The PAF of these mRNAs has been calculated in the simulation. Therefore the concentration of the polysomes with 4 and 5 ribosomes bound has been divided by the total concentration of the corresponding mRNA. This total concentration did not change during the simulation. In addition, this fraction has been multiplied by 50, since the polysomal concentration is always smaller than the total in this model. This factor 50 has been chosen arbitrarily, but is needed because in the analysis the polysomal fraction can have a higher concentration of a certain mRNA than the total fraction. This is because the polysomal mRNA is concentrated in the measurements, while the polysomal mRNA has of course always a lower concentration than the total mRNA in the model.

The initiation rates of the different mRNA classes have been chosen, in a way that they give a high, a middle, and a low PAF value. The simulation result for the PAF values of the three groups is displayed in Figure 5.2.

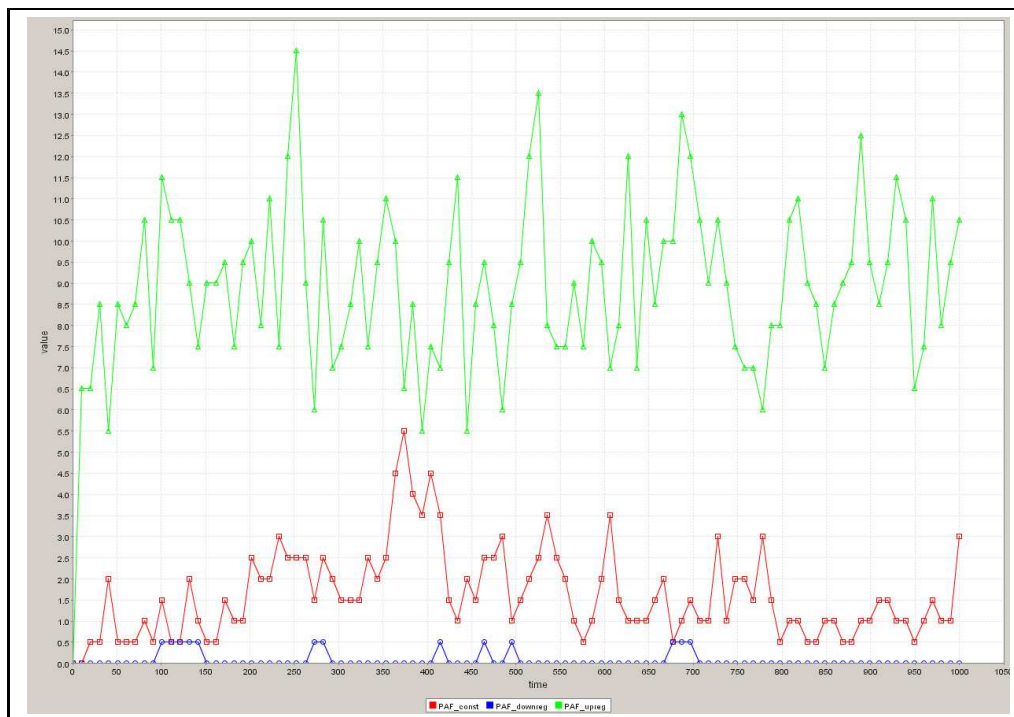


Figure 5.2: Simulation of the PAF value for a bitstring model with three different types of mRNA (upregulated, downregulated, not regulated)



Figure 5.3: Simulation bitstring model upregulated mRNA

It has to be pointed out that the values in Figure 5.1 are delta PAF values, and denote a temporal change of the translation state. Since in this simulation only a steady state is considered, it can not be compared directly to the delta PAFs. One could derive delta PAFs from this model by implementing a temporal change in the initiation rates and taking the fraction of the PAFs at different time points. This simulation was only meant to illustrate the polysomal distributions, which lead to different PAF values. Therefore the polysomal profiles of the different mRNA classes in this simulation are shown in Figures 5.3, 5.4, and 5.5. As already mentioned, the initiation rates have been chosen in way, that the PAF distribution forms three different classes. Figure 5.3 shows the upregulated class with a PAF of about 8 (no logarithmic scale). As one would expect, most of the mRNAs in this class have 5 ribosomes bound. Figure 5.4 shows the simulation for the downregulated class, which has a PAF of about 0.1, and forms an adverse distribution where the highest concentration is made up by untranslated mRNA. Figure 5.5 shows the simulation result for the mRNA class which has a PAF at around 1, that has not been regulated. In addition, this simulation shows that the stochastic noise is bigger in the PAF values, than in the mRNA concentrations.



Figure 5.4: Simulation bitstring model downregulated mRNA

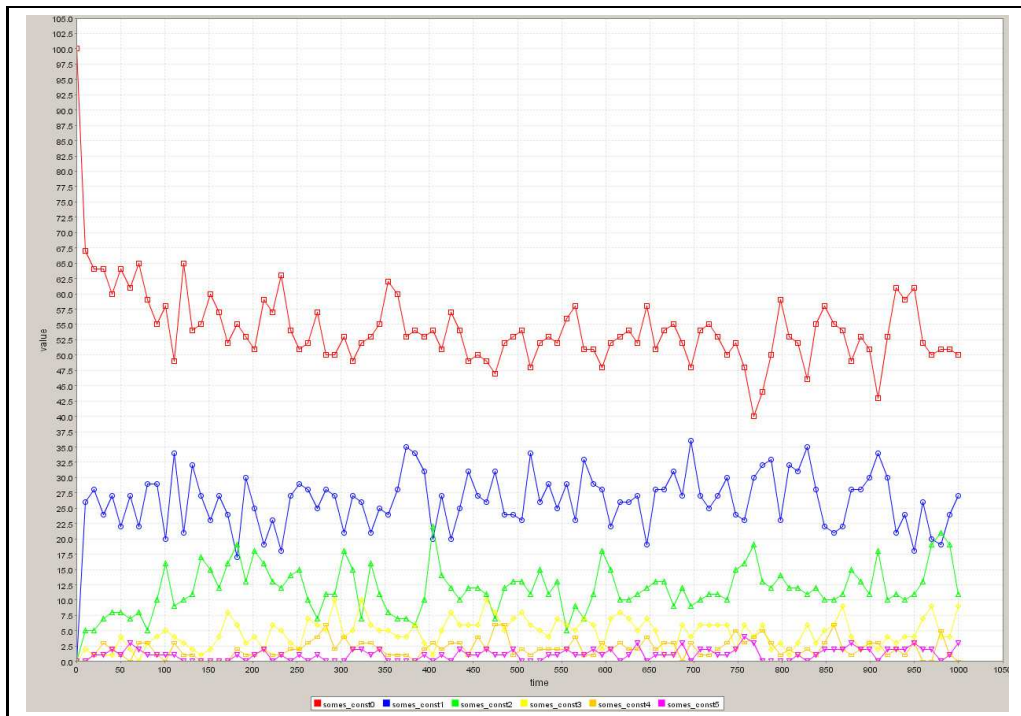


Figure 5.5: Simulation bitstring model not regulated mRNA

5.3 Conclusions

In this work three different approaches to model the occupancy of mRNA with ribosomes have been developed. It has been shown that a simple model where the ribosomes just associate with a certain rate, and dissociate with another rate, can not explain the osmotic shock response of the polysomal profiles. In addition, a model where the number of bound ribosomes influences the binding of other ribosomes has been developed. This model is able to describe different steady states of polysomal profiles, but requires many parameters. A third model that takes the binding positions of the ribosomes into account has been developed, but it could not be tested well enough, since this model is computationally very demanding,

Different possible explanations for the osmotic shock response have been tested with these models. While a degradation of ribosomes, or an increase of mRNA seem unlikely to cause the shift from polysomes to monosomes, the tested models favors a regulation of the initiation. Nonetheless, the developed models were altogether not capable of mimicking the response shown in the data. This indicates that either some important points are not considered in the models, or the method used to fit the models to the data was not appropriate. A problem arising from the method of measuring the data is that no value is given for the concentrations of the polysomes consisting of more than 10 ribosomes. This forms a restriction for fitting the models to the data. Additional assumptions to be included in the models could be different ways of regulating the initiation (step function, exponential decrease), a regulation of the dissociation, or different sets of coordinately regulated polysomes (groups as in the three initiation rate model). In addition, one could work on a method to make the bitstring model feasible for computational simulation, for instance by scaling the data down to a lower number of maximal bound ribosomes, by implementing it with a faster method, or by simplifying the model in some way.

Appendix A

Proofs

A.1 Derivation of fomulae (3.5) and (3.6)

To proof (3.5) it has to be shown that:

$$M_i = M_{i-1} \cdot X = M_{i-1} \cdot \frac{ka \cdot R}{kd} \quad (\text{A.1})$$

Proof by induction:

1. Basis

from Equation (3.1) and the steady state condition follows:

$$\begin{aligned} 0 &= -ka \cdot M_0 \cdot R + kd \cdot M_1 \\ \Leftrightarrow M_1 &= M_0 \cdot \frac{ka \cdot R}{kd} \end{aligned} \quad (\text{A.2})$$

2. Inductive hypothesis

(A.1)

3. Step

From Equation (3.2) and the steady state condition follows:

$$\begin{aligned} 0 &= ka \cdot M_{i-1} \cdot R - kd \cdot M_i - ka \cdot M_i \cdot R + kd \cdot M_{i+1} \\ \Leftrightarrow M_{i+1} &= M_{i-1} \cdot \frac{ka \cdot R}{kd} - M_i - M_i \cdot \frac{ka \cdot R}{kd} \\ \stackrel{(\text{A.1})}{\Leftrightarrow} M_{i+1} &= \frac{ka \cdot M_{i-1} \cdot R}{kd} - M_{i-1} \cdot \frac{ka \cdot R}{kd} - \frac{ka \cdot M_i \cdot R}{kd} \\ \Leftrightarrow M_{i+1} &= M_i \frac{ka \cdot R}{kd} \end{aligned}$$

Therefore is

$$M_i = M_0 \cdot \left(\frac{ka \cdot R}{kd} \right)^i = M_0 \cdot X^i \quad (\text{A.3})$$

An expression that depends on the total mRNA rather than on the unbound mRNA can be deduced by solving the sum over all translation states for M_0

$$\begin{aligned}
M_{tot} &= \sum_{i=0}^N M_i \\
\Leftrightarrow M_{tot} &= \sum_{i=0}^N M_0 \cdot X^i \\
\Leftrightarrow \frac{M_{tot}}{M_0} &= \sum_{i=0}^N X^i = \frac{X^{N+1} - 1}{X - 1} \\
\Leftrightarrow M_0 &= \frac{M_{tot}(X - 1)}{X^{N+1} - 1}
\end{aligned} \tag{A.4}$$

Combining Equations (A.3) and (A.4) yields:

$$M_i = \frac{M_{tot}(X - 1)}{X^{N+1} - 1} X^i \tag{A.5}$$

A.2 Derivation of formula (3.7)

The proof of Equation (3.7) is analog to the proof of formula (3.5). The rate equations for this system read:

$$\frac{d}{dt} M_0 = -ka_0 \cdot M_0 \cdot R + kd \cdot M_1 \tag{A.6}$$

$$\frac{d}{dt} M_i = ka_{i-1} \cdot M_{i-1} \cdot R - kd \cdot M_i - ka_i \cdot M_i \cdot R + kd \cdot M_{i+1} \tag{A.7}$$

$$\frac{d}{dt} M_N = ka_{N-1} \cdot M_{N-1} \cdot R - kd \cdot M_N \tag{A.8}$$

$$\frac{d}{dt} R = \sum_{i=1}^N (-ka_{i-1} \cdot M_{i-1} \cdot R + kd \cdot M_i) \tag{A.9}$$

What has to be shown is:

$$M_i = M_{i-1} \cdot ka_{i-1} \cdot \frac{R}{kd} \tag{A.10}$$

1. Basis

$$\begin{aligned}
\text{(A.6)} \Rightarrow 0 &= -ka_0 \cdot M_0 \cdot R + kd \cdot M_1 \\
\Leftrightarrow M_1 &= M_0 \cdot ka_0 \cdot \frac{R}{kd}
\end{aligned} \tag{A.11}$$

2. Inductive hypothesis

(A.10)

3. Step

$$\begin{aligned} \text{(A.7)} \Rightarrow 0 &= ka_{i-1} \cdot M_{i-1} \cdot R - kd \cdot M_i - ka_i \cdot M_i \cdot R + kd \cdot M_{i+1} \\ &\Leftrightarrow M_{i+1} = -ka_{i-1} \cdot M_{i-1} \cdot \frac{R}{kd} + M_i + ka_i \cdot M_i \cdot \frac{R}{kd} \\ \stackrel{\text{(A.10)}}{\Leftrightarrow} M_{i+1} &= -ka_{i-1} \cdot M_{i-1} \cdot \frac{R}{kd} + M_{i-1} \cdot ka_{i-1} \cdot \frac{R}{kd} + ka_i \cdot M_i \cdot \frac{R}{kd} \\ &\Leftrightarrow M_{i+1} = ka_i \cdot M_i \cdot \frac{R}{kd} \end{aligned} \tag{A.12}$$

From (A.12) it follows that (3.7) is true.

Appendix B

Deterministic simulation in MATLAB

The change over time of the concentrations of the species in a biochemical system can be described by a set of ordinary differential equations (ODEs). The change of each species at a specific time point can be expressed by a gradient function that depends on all other concentrations, on the parameters and on the time.

$$\frac{d}{dt}X_i = f_i(X_1, \dots, X_M, p_1, \dots, p_k, t), \quad i = 1 \dots M \quad (\text{B.1})$$

A general way to derive ODEs for a biochemical system is described in the introduction. A way to simulate a system is to integrate these equations for certain parameters and initial concentrations numerically. Numerically integrating a system means to repetitively calculate the gradient of the single rate model, and update the system values accordingly. This gives an approximation of how the system would evolve.

To numerically integrate a system in MATLAB a function is required, that calculates the gradient from the present metabolite concentrations and parameters. A function that does this for the single rate model with maximum of 10 bound ribosomes is given Figure B.1. This function calculates the gradient of the system according to Equations (3.1), (3.2), (3.3), and (3.4) and takes the time t , the concentration vector x and the parameter vector p as input. To make a simulation with this gradient function one needs to specify initial concentration values and a set of parameters. Figure B.2 gives an example how this is done in MATLAB. The plot that is produced by this function is shown in figure 3.3. Because some of the reactions may be fast in the beginning, where the system converges toward a steady state, the stiff ODE solver *ode15s* was used. The different ODE solvers included in MATLAB are listed in the MATLAB documentation ¹.

¹<http://www.mathworks.com/access/helpdesk/help/techdoc/ref/ode15s.html>

```

function dx = gradient(t,x,p)
    ka = p(1); % define parameters
    kd = p(2);

    R = x(12); % define ribosome concentration
    dx = zeros(12,1); % initialize gradient

    % calculate rate of change for each mRNA
    dx(1) = -ka*x(1)*R + kd*x(2);
    dx(2) = -ka*x(2)*R - kd*x(2) + ka*x(1)*R + kd*x(3);
    dx(3) = -ka*x(3)*R - kd*x(3) + ka*x(2)*R + kd*x(4);
    dx(4) = -ka*x(4)*R - kd*x(4) + ka*x(3)*R + kd*x(5);
    dx(5) = -ka*x(5)*R - kd*x(5) + ka*x(4)*R + kd*x(6);
    dx(6) = -ka*x(6)*R - kd*x(6) + ka*x(5)*R + kd*x(7);
    dx(7) = -ka*x(7)*R - kd*x(7) + ka*x(6)*R + kd*x(8);
    dx(8) = -ka*x(8)*R - kd*x(8) + ka*x(7)*R + kd*x(9);
    dx(9) = -ka*x(9)*R - kd*x(9) + ka*x(8)*R + kd*x(10);
    dx(10) = -ka*x(10)*R - kd*x(10) + ka*x(9)*R + kd*x(11);
    dx(11) = ka*x(10)*R - kd*x(11);

    % calculate rate for ribosomes
    dx(12) = - ka*x(1)*R - ka*x(2)*R - ka*x(3)*R - ka*x(4)*R
    - ka*x(5)*R - ka*x(6)*R - ka*x(7)*R - ka*x(8)*R - ka*x(9)*R -
    ka*x(10)*R + kd*x(2) + kd*x(3) + kd*x(4) + kd*x(5) + kd*x(6)+ kd*x(7)
    + kd*x(8) + kd*x(9) + kd*x(10) + kd*x(11);

```

Figure B.1: MATLAB code to calculate the gradient for the single rate model with $N = 10$

```

% set ka to 0.0015 and kd to 1
p = [ 0.0015 1];

% set initial concentrations M0, M1, ..., M10, R
start_x = [ 10 0 0 0 0 0 0 0 0 0 0 0 1500];

% options for the ODE solver
options = odeset( 'RelTol', 1e-4, 'AbsTol', [1e-4]*ones(1,12) );

% integrate the gradient function for the time interval [0 20]
[T,Y] = ode15s( @gradient, [0 20], start_x, options, p );

% plot the time course
plot( T,Y(:,1), T,Y(:,2), T,Y(:,3), T,Y(:,4), T,Y(:,5), T,Y(:,6),
T,Y(:,7), T,Y(:,8), T,Y(:,9), T,Y(:,10), T,Y(:,11))

```

Figure B.2: MATLAB code to integrate the gradient function in a certain interval for certain parameters and start values

Bibliography

- Abel, N. (1826). Beweis der Unmöglichkeit algebraische Gleichungen von höheren Graden als dem vierten allgemein aufzulösen. *J. reine angew. Math*, 1:65–84.
- Alberts, B., Johnson, A., Lewis, J., Raff, M., Roberts, K., and P., W. (2002). *Molecular Biology of the Cell*. Garland Science.
- Albertyn, J., Hohmann, S., and Prior, B. (1994). Characterization of the osmotic-stress response in *Saccharomyces cerevisiae*: osmotic stress and glucose repression regulate glycerol-3-phosphate dehydrogenase independently. *Current Genetics*, 25(1):12–18.
- Arava, Y., Wang, Y., Storey, J. D., Liu, C. L., Brown, P. O., and Herschlag, D. (2003). Genome-wide analysis of mRNA translation profiles in *Saccharomyces cerevisiae*. *Proc Natl Acad Sci U S A*, 100(7):3889–3894.
- Ashe, M., De Long, S., and Sachs, A. (2000). Glucose Depletion Rapidly Inhibits Translation Initiation in Yeast. *Molecular Biology of the Cell*, 11:833–848.
- Bentley, D. (1995). Regulation of transcriptional elongation by RNA polymerase II. *Curr. Opin. Genet. Dev*, 5:210–216.
- Bernstein, P. and Ross, J. (1989). Poly(A), poly(A) binding protein and the regulation of mRNA stability. *Trends Biochem Sci*, 14(9):373–377.
- Black, D. L. (2000). Protein diversity from alternative splicing: A challenge for bioinformatics and post-genome biology. *Cell*.
- Blomberg, A. and Adler, L. (1992). Physiology of osmotolerance in fungi. *Adv Microb Physiol*, 33:145–212.
- Brown, V., Jin, P., Ceman, S., Darnell, J., ODonnell, W., Tenenbaum, S., Jin, X., Feng, Y., Wilkinson, K., Keene, J., et al. (2001). Microarray identification of FMRP-associated brain mRNAs and altered mRNA translational profiles in fragile X syndrome. *Cell*, 107(4):477–487.
- Causton, H., Ren, B., Koh, S., Harbison, C., Kanin, E., Jennings, E., Lee, T., True, H., Lander, E., and Young, R. (2001). Remodeling of Yeast Genome Expression in Response to Environmental Changes. *Molecular Biology of the Cell*, 12:323–337.

- Conaway, R. C. and Conaway, J. W. (1993). General initiation factors for RNA polymerase II. *Annu Rev Biochem*, 62:161–190.
- Daneholt, B. (1997). A look at messenger RNP moving through the nuclear pore. *Cell*, 88(5):585–588.
- Deschenes, R. J., Lin, H., Ault, A. D., and Fassler, J. S. (1999). Antifungal properties and target evaluation of three putative bacterial histidine kinase inhibitors. *Antimicrob Agents Chemother*, 43(7):1700–1703.
- Dickson, L. (1998). mRNA translation in yeast during entry into stationary phase. *Molecular and General Genetics MGG*, 259(3):282–293.
- Ding, D. and Lipshitz, H. (1993). Localized RNAs and their functions. *Bioessays*, 15(10):651–8.
- Drummond, D. R., Armstrong, J., and Colman, A. (1985). The effect of capping and polyadenylation on the stability, movement and translation of synthetic messenger RNAs in *Xenopus* oocytes. *Nucleic Acids Res*, 13(20):7375–7394.
- Eddy, S. R. (1999). Noncoding RNA genes. *Curr Opin Genet Dev*, 9(6):695–699.
- Estruch, F. (2000). Stress-controlled transcription factors, stress-induced genes and stress tolerance in budding yeast. *FEMS Microbiol Rev*, 24(4):469–86.
- Finney, A. and Hucka, M. (2003). Systems biology markup language: Level 2 and beyond. *Biochem Soc Trans*, 31(Pt 6):1472–1473.
- Francois, J. and Parrou, J. (2001). Reserve carbohydrates metabolism in the yeast *Saccharomyces cerevisiae*. *FEMS Microbiol Rev*, 25(1):125–45.
- Gasch, A., Spellman, P., Kao, C., Carmel-Harel, O., Eisen, M., Storz, G., Botstein, D., and Brown, P. (2000). Genomic Expression Programs in the Response of Yeast Cells to Environmental Changes. *Science's STKE*, 11(12):4241–4257.
- Gibson, M. and Bruck, J. (2000). Efficient exact stochastic simulation of chemical systems with many species and many channels. *J. Phys. Chem. A*, 104(9):1876–1889.
- Gillespie, D. (1977). Exact stochastic simulation of coupled chemical reactions. *The Journal of Physical Chemistry*, 81(25):2340–2361.
- Goffeau, A., Barrell, B. G., Bussey, H., Davis, R. W., Dujon, B., Feldmann, H., Galibert, F., Hoheisel, J. D., Jacq, C., Johnston, M., Louis, E. J., Mewes, H. W., Murakami, Y., Philippsen, P., Tettelin, H., and Oliver, S. G. (1996). Life with 6000 genes. *Science*, 274(5287):563–567.
- Gurdon, J. B. (1968). Changes in somatic cell nuclei inserted into growing and maturing amphibian oocytes. *J Embryol Exp Morphol*, 20(3):401–414.

- Heinrich, R. and Rapoport, T. (1974). A linear steady-state treatment of enzymatic chains. General properties, control and effector strength. *Eur J Biochem*, 42(1):89–95.
- Helliwell, S., Wagner, P., Kunz, J., Deuter-Reinhard, M., Henriquez, R., and Hall, M. (1994). TOR1 and TOR2 are structurally and functionally similar but not identical phosphatidylinositol kinase homologues in yeast. *Mol. Biol. Cell*, 5:105–118.
- Herrick, D., Parker, R., and Jacobson, A. (1990). Identification and comparison of stable and unstable mRNAs in *Saccharomyces cerevisiae*. *Molecular and Cellular Biology*, 10(5):2269–2284.
- Hirayama, T., Maeda, T., Saito, H., and Shinozaki, K. (1995). Cloning and characterization of seven cDNAs for hyperosmolarity-responsive (HOR) genes of *Saccharomyces cerevisiae*. *Molecular Genetics and Genomics*, 249(2):127–138.
- Hohmann, S. (2002). Osmotic stress signaling and osmoadaptation in yeasts. *Microbiol Mol Biol Rev*, 66(2):300–372.
- Hounsa, C. G., Brandt, E. V., Thevelein, J., Hohmann, S., and Prior, B. A. (1998). Role of trehalose in survival of *Saccharomyces cerevisiae* under osmotic stress. *Microbiology*, 144 (Pt 3):671–680.
- Huang, Y. and Carmichael, G. C. (1996). Role of polyadenylation in nucleocytoplasmic transport of mRNA. *Mol Cell Biol*, 16(4):1534–1542.
- Jackson, R. and Wickens, M. (1997). Translational controls impinging on the 5'-untranslated region and initiation factor proteins. *Curr. Opin. Genet. Dev*, 7(2):233–241.
- Jacobson, A., Brown, A., Donahue, J., Herrick, D., Parker, R., and Peltz, S. (1990). Regulation of mRNA stability in yeast. *NATO ASI Ser. Ser. H*, 49:45–54.
- Jacobson, A. and Peltz, S. (1996). Interrelationships of the Pathways of mRNA Decay and Translation in Eukaryotic Cells. *Annual Review of Biochemistry*, 65(1):693–739.
- Johannes, G., Carter, M., Eisen, M., Brown, P., and Sarnow, P. (1999). Identification of eukaryotic mRNAs that are translated at reduced cap binding complex eIF4F concentrations using a cDNA microarray. *Proceedings of the National Academy of Sciences*, 96(23):13118–13123.
- Kacser, H. and Burns, J. (1973). The control of flux. *Symp. Soc. Exp. Biol*, 27(65):104.
- Kimball, S. (2001). Regulation of translation initiation by amino acids in eukaryotic cells. *Prog Mol Subcell Biol*, 26:155–84.
- Kingston, R. (1999). ATP-dependent remodeling and acetylation as regulators of chromatin fluidity. *Genes & Development*, 13(18):2339–2352.

- Kitano, H. (2002). Systems Biology: A Brief Overview. *Science*, 295(5560):1662–1664.
- Klipp, E., Herwig, R., Kowald, A., Wierling, C., and Lehrach, H. (2005a). *Systems Biology in Practice: Concepts, Implementation and Application*. John Wiley & Sons.
- Klipp, E., Nordlander, B., Kruger, R., Gennemark, P., and Hohmann, S. (2005b). Integrative model of the response of yeast to osmotic shock. *Nat Biotechnol*, 23(8):975–982. Evaluation Studies.
- Kornberg, R. (1999). Eukaryotic transcriptional control. *Trends Cell Biol*, 9(12):M46–9.
- Kuhn, K. M., DeRisi, J. L., Brown, P. O., and Sarnow, P. (2001). Global and specific translational regulation in the genomic response of *Saccharomyces cerevisiae* to a rapid transfer from a fermentable to a nonfermentable carbon source. *Mol Cell Biol*, 21(3):916–927.
- Lewis, J. D. and Tollervey, D. (2000). Like attracts like: getting RNA processing together in the nucleus. *Science*, 288(5470):1385–1389.
- Lindahl, L. and Hinnebusch, A. (1992). Diversity of mechanisms in the regulation of translation in prokaryotes and lower eukaryotes. *Curr Opin Genet Dev*, 2(5):720–6.
- Lowell, J. E., Rudner, D. Z., and Sachs, A. B. (1992). 3'-UTR-dependent deadenylation by the yeast poly(A) nuclease. *Genes Dev*, 6(11):2088–2099.
- Luyten, K., Albertyn, J., Skibbe, W., Prior, B., Ramos, J., Thevelein, J., and Hohmann, S. (1995). Fps1, a yeast member of the MIP family of channel proteins, is a facilitator for glycerol uptake and efflux and is inactive under osmotic stress. *EMBO J*, 14(7):1360–1371.
- MacKay, V. L., Li, X., Flory, M. R., Turcott, E., Law, G. L., Serikawa, K. A., Xu, X. L., Lee, H., Goodlett, D. R., Aebersold, R., Zhao, L. P., and Morris, D. R. (2004). Gene expression analyzed by high-resolution state array analysis and quantitative proteomics: response of yeast to mating pheromone. *Mol Cell Proteomics*, 3(5):478–489.
- Mata, J., Marguerat, S., and Bahler, J. (2005). Post-transcriptional control of gene expression: a genome-wide perspective. *Trends Biochem Sci*, 30(9):506–514.
- Matlab, U. (2005). The Mathworks Inc. *Natick, MA*.
- McCarthy, J. and Kollmus, H. (1995). Cytoplasmic mRNA-protein interactions in eukaryotic gene expression. *Trends Biochem Sci*, 20(5):191–7.
- McCarthy, J. E. (1998). Posttranscriptional control of gene expression in yeast. *Microbiol Mol Biol Rev*, 62(4):1492–1553.
- Mikulits, W., Pradet-Balade, B., Habermann, B., Beug, H., Garcia-Sanz, J. A., and Mullner, E. W. (2000). Isolation of translationally controlled mRNAs by differential screening. *FASEB J*, 14(11):1641–1652.

- Muhlrad, D., Decker, C., and Parker, R. (1995). Turnover mechanisms of the stable yeast PGK1 mRNA. *Molecular and Cellular Biology*, 15(4):2145–2156.
- Nairn, A. and Palfrey, H. (1996). Regulation of protein synthesis by calcium. *Translational Control*, pages 295–318.
- Norbeck, J., Pählman, A., Akhtar, N., Blomberg, A., and Adler, L. (1996). Purification and Characterization of Two Isoenzymes of DL-Glycerol-3-phosphatase from *Saccharomyces cerevisiae*. *Journal of Biological Chemistry*, 151(9):2987–2999.
- Nwaka, S., Mechler, B., Destruelle, M., and Holzer, H. (1995). Phenotypic features of trehalase mutants in *Saccharomyces cerevisiae*. *FEBS Lett*, 360(3):286–90.
- Pain, V. (1996). Initiation of protein synthesis in eukaryotic cells. *FEBS Journal*, 236:747–771.
- Prieto, S., Bernard, J., and Scheffler, I. (2000). Glucose-regulated Turnover of mRNA and the Influence of Poly (A) Tail Length on Half-life. *Journal of Biological Chemistry*, 275(19):14155–14166.
- Ptushkina, M., von der Haar, T., Vasilescu, S., Frank, R., Birkenhager, R., and McCarthy, J. (1998). Cooperative modulation by eIF4G of eIF4E-binding to the mRNA 5'cap in yeast involves a site partially shared by p20. *EMBO J*, 17(16):4798–808.
- Raitt, D. et al. (2000). Yeast Cdc 42 GTPase and Ste 20 PAK-like kinase regulate Sho 1-dependent activation of the Hog 1 MAPK pathway. *The EMBO Journal*, 19(17):4623–4631.
- Ramsey, S., Orrell, D., and Bolouri, H. (2005). Dizzy: stochastic simulation of large-scale genetic regulatory networks. *J. Bioinf. Comp. Biol*, 3(2):415–436.
- Saavedra, C., Tung, K., Amberg, D., Hopper, A., and Cole, C. (1996). Regulation of mRNA export in response to stress in *Saccharomyces cerevisiae*. *Genes Dev*, 10(13):1608–20.
- Serikawa, K. A., Xu, X. L., MacKay, V. L., Law, G. L., Zong, Q., Zhao, L. P., Bumgarner, R., and Morris, D. R. (2003). The transcriptome and its translation during recovery from cell cycle arrest in *Saccharomyces cerevisiae*. *Mol Cell Proteomics*, 2(3):191–204.
- Shapiro, B. (2004). MathSBML: a package for manipulating SBML-based biological models. *Bioinformatics*, 20(16):2829–2831.
- Singer, M. and Lindquist, S. (1998). Multiple effects of trehalose on protein folding in vitro and in vivo. *Mol Cell*, 1(5):639–48.
- Singer, R. (1992). The cytoskeleton and mRNA localization. *Curr Opin Cell Biol*, 4(1):15–9.
- Sonenberg, N. (1996). mRNA 5' cap-binding protein eIF4E and control of cell growth+ In: Hershey JWB, Mathews MB, Sonenberg N, eds+ Translational control+ Cold Spring Harbor.

- Southern, E. M. (2001). DNA microarrays. History and overview. *Methods Mol Biol*, 170:1–15.
- Storn, R. and Price, K. (1997). Differential Evolution—A Simple and Efficient Heuristic for global Optimization over Continuous Spaces. *Journal of Global Optimization*, 11(4):341–359.
- Swaminathan, S., Masek, T., Molin, C., Pospisek, M., and Sunnerhagen, P. (2006). Rck2 is required for reprogramming of ribosomes during oxidative stress. *Mol Biol Cell*, 17(3):1472–1482.
- Tamas, M., Luyten, K., Sutherland, F., Hernandez, A., Albertyn, J., Valadi, H., Li, H., Prior, B., Kilian, S., Ramos, J., et al. (1999). Fps 1 p controls the accumulation and release of the compatible solute glycerol in yeast osmoregulation. *Molecular Microbiology*, 31(4):1087–1104.
- Teige, M., Scheikl, E., Reiser, V., Ruis, H., and Ammerer, G. (2001). Rck2, a member of the calmodulin-protein kinase family, links protein synthesis to high osmolarity MAP kinase signaling in budding yeast. *Proceedings of the National Academy of Sciences*, 98(10):5625–5630.
- Warner, J. (1999). The economics of ribosome biosynthesis in yeast. *Trends Biochem. Sci*, 24(11):437–440.
- Wek, R. (1994). eIF-2 kinases: regulators of general and gene-specific translation initiation. *Trends Biochem Sci*, 19(11):491–6.
- Widmann, C., Gibson, S., Jarpe, M. B., and Johnson, G. L. (1999). Mitogen-activated protein kinase: conservation of a three-kinase module from yeast to human. *Physiol Rev*, 79(1):143–180.
- Wilhelm, J. and Vale, R. (1993). RNA on the move: the mRNA localization pathway. *J Cell Biol*, 123(2):269–74.
- Wilson, M., Sawicki, S., White, P., and Darnell Jr, J. (1978). A correlation between the rate of poly (A) shortening and half-life of messenger RNA in adenovirus transformed cells. *J Mol Biol*, 126(1):23–36.
- Wolfram, S. (2003). *The Mathematica Book*, 5. Auflage. Wolfram Media, Champaign (IL).
- Wood, J. M. (1999). Osmosensing by bacteria: signals and membrane-based sensors. *Microbiol Mol Biol Rev*, 63(1):230–262.
- Zi, Z. and Klipp, E. (2006). Sbml-pet: A systems biology markup language based parameter estimation tool (submitted).
- Zingg, H. H., Lefebvre, D. L., and Almazan, G. (1988). Regulation of poly(A) tail size of vasopressin mRNA. *J Biol Chem*, 263(23):11041–11043.

Zong, Q., Schummer, M., Hood, L., and Morris, D. (1999). Messenger RNA translation state: The second dimension of high-throughput expression screening. *Proceedings of the National Academy of Sciences*, 96(19):10632–10636.

Selbstständigkeitserklärung

Hiermit erkläre ich, die vorliegende Arbeit selbstständig ohne fremde Hilfe verfaßt und nur die angegebene Literatur und Hilfsmittel verwendet zu haben.

Jannis Uhlendorf
1. August 2006